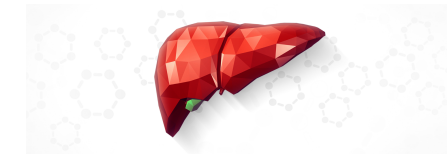


Physiological models for the analysis of liver function (PKPD models)

Matthias König

LiSyM Systems Medicine of the Liver
Humboldt University Berlin, Institute for Theoretical Biology
livermetabolism.com

Liver Function Tests



Liver specific clearance of substance

- Galactose elimination capacity (GEC)
- Caffeine clearance
- LiMAX Test (Methacetin)

Evaluation of liver function

- Transplantation, Hepatectomy, Liver disease

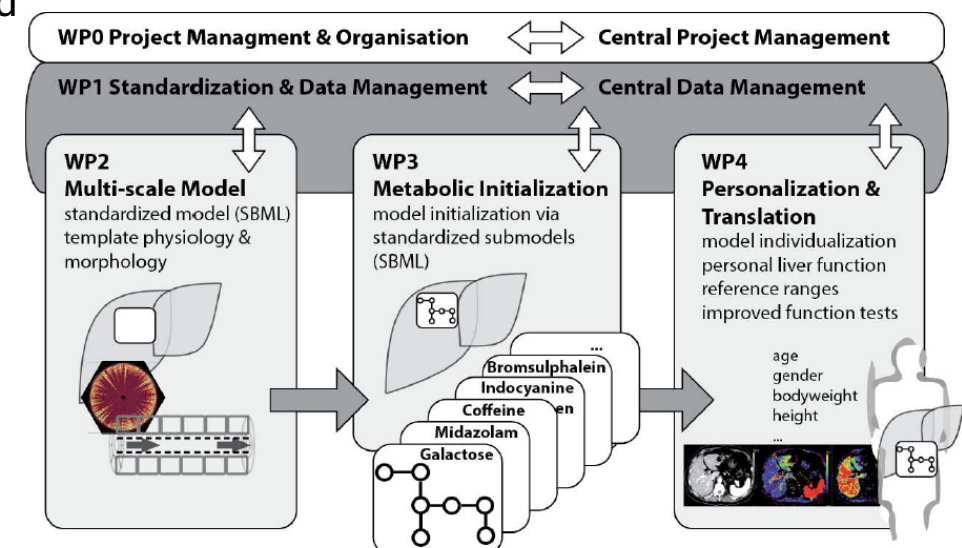
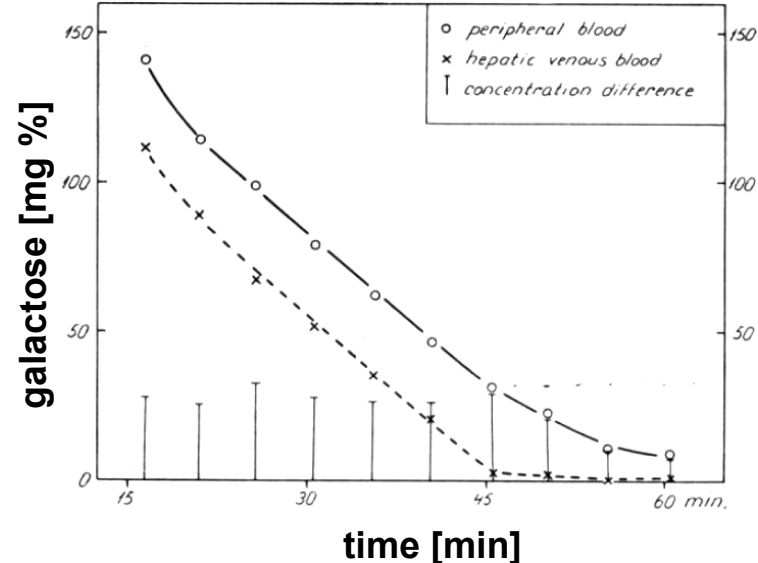
Analysis via simple cutoff

- No account for large variability in liver volume, blood flow, organ volumes, expression
 - age, gender, bodyweight, height, ...

=> personalized physiological models (*in silico* trials)

- None of the liver specific information used for evaluation
 - morphology, perfusion, metabolism, ultrastructure, ...

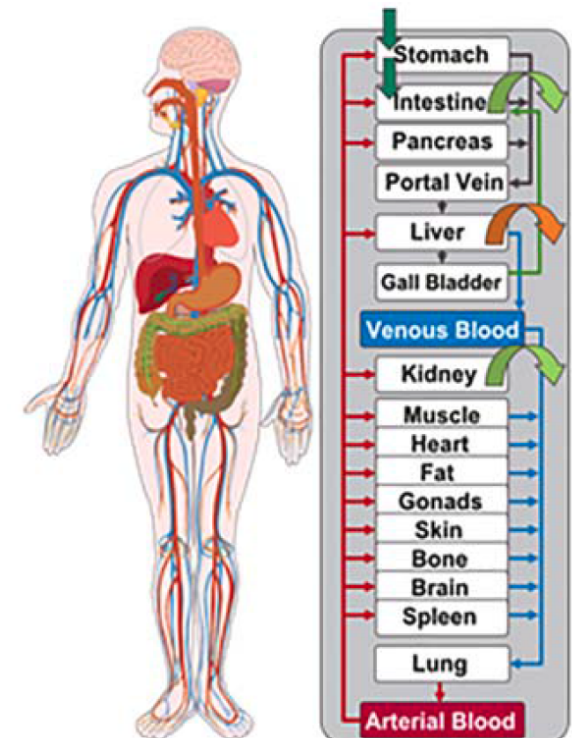
=> detailed kinetic multiscale models



Vilstrup1974

What are PKPD models?

- PKPD
 - **PharmacoKinetics**: determines fate of substances administered to organism
 - **PharmacoDynamics** is the study of how the drug affects the organism
- PKPD Models
 - human/animal physiology in the computer
 - combine information on the drug with knowledge on the physiology and biology at organism level
 - Specific models for certain drugs & substances
 - contain explicit representation of the organs most relevant for **Absorption, Distribution, Metabolism, Elimination (ADME)**
 - **Tissues are linked by arterial and venous blood compartments** characterized by associated blood flow rates, tissue-partition coefficient , and permeability
 - Minimal models: often no blood flow, small set of compartments



PKPD Applications

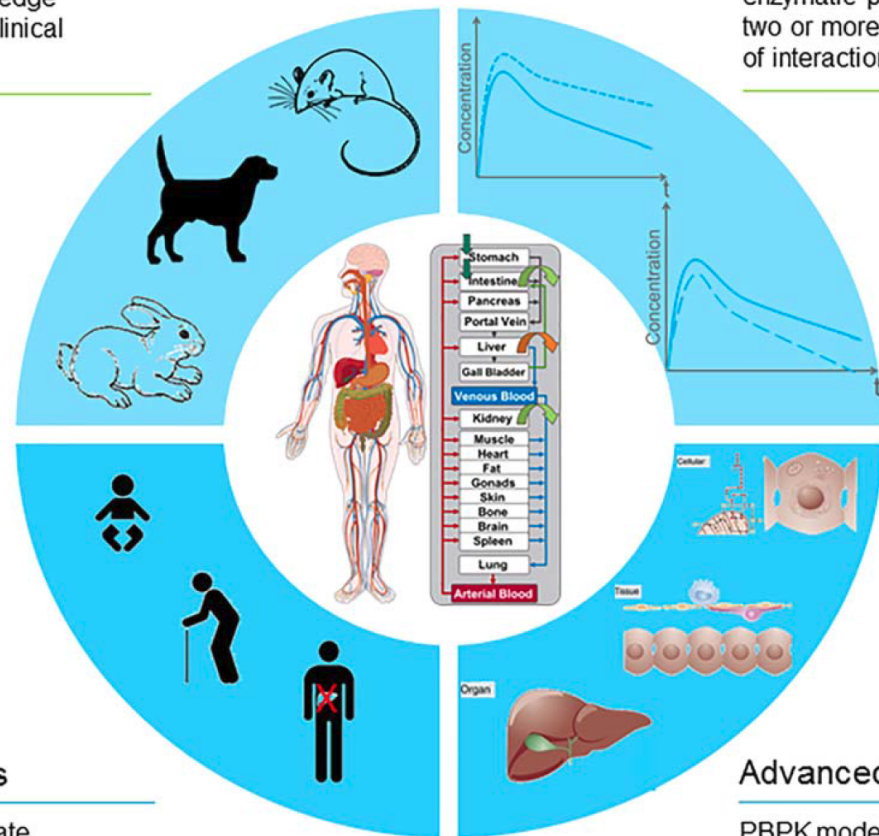
Cross-Species Extrapolation

PBPK models can be used to facilitate the extrapolation of knowledge generated in various preclinical species to humans



Special Populations

By including the appropriate physiological information, PBPK models can be used to make predictions in special populations



Drug Drug Interactions (DDI)

Thanks of the explicit inclusion of enzymatic processes, the combination of two or more models allow the prediction of interaction between drugs

Individual Dosing

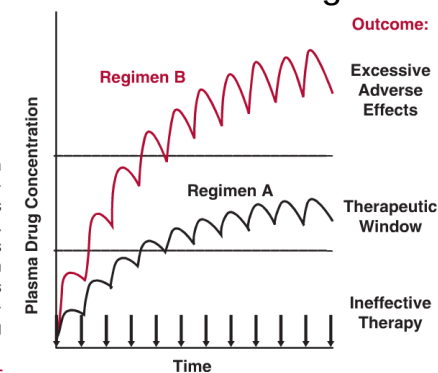


FIGURE 1-4. When a drug is given in a fixed dose and at fixed time intervals (denoted by the arrows), it accumulates within the body until a plateau is reached. With regimen A, therapeutic success is achieved although not initially. With regimen B, the therapeutic objective is achieved more quickly, but the drug concentration is ultimately too high, resulting in excessive adverse effects.

Advanced Applications

PBPK models can also be integrated in more complex models such as multiscale modelling or statistical modelling, using methods such as Bayesian approaches

Figure 3 Schematic representation of the most common applications of PBPK modeling.

Building blocks of a PBPK model

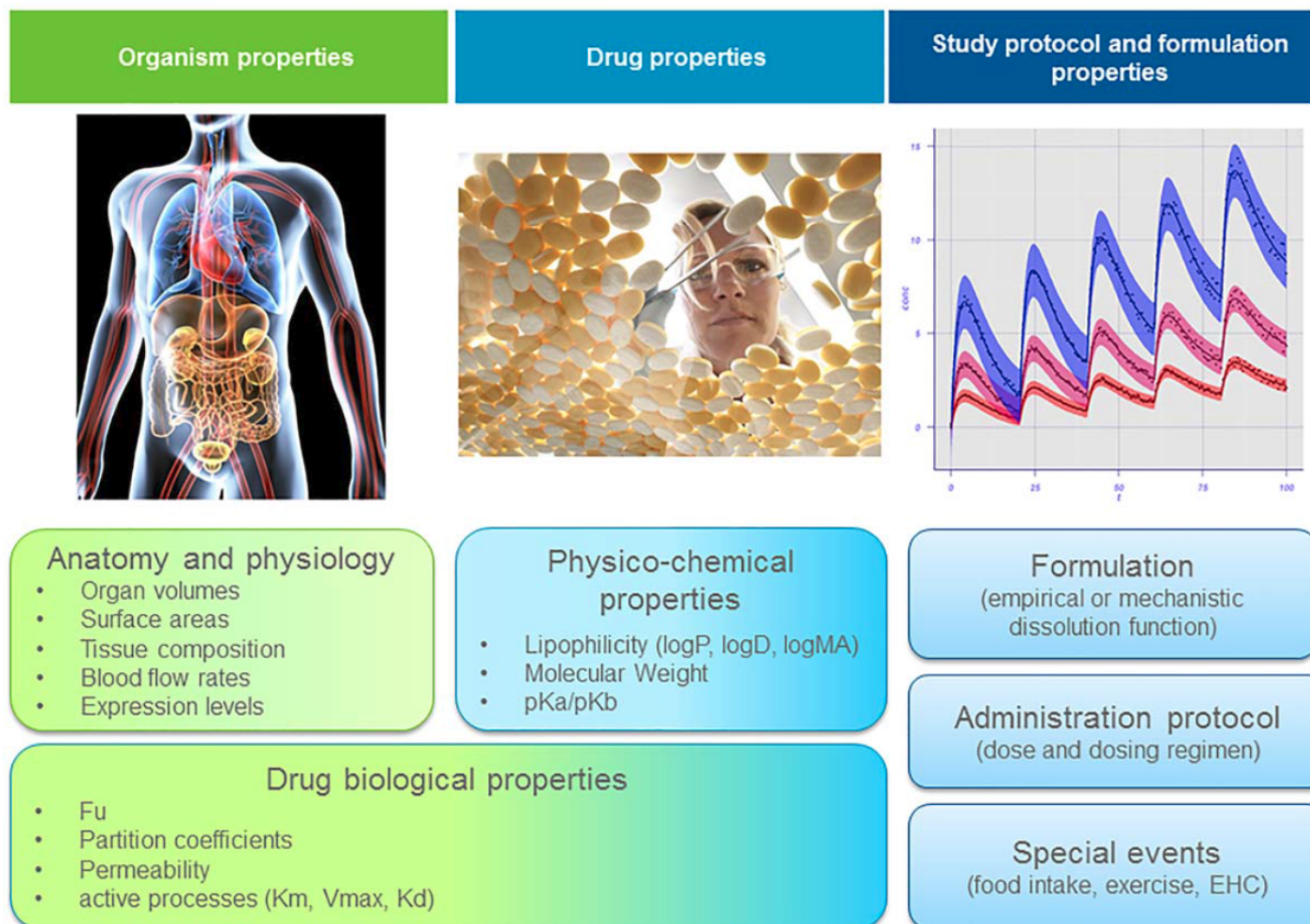


Figure 2 Representation of the general building blocks which can be part of a PBPK model. Some components may be optional depending on the model considered.

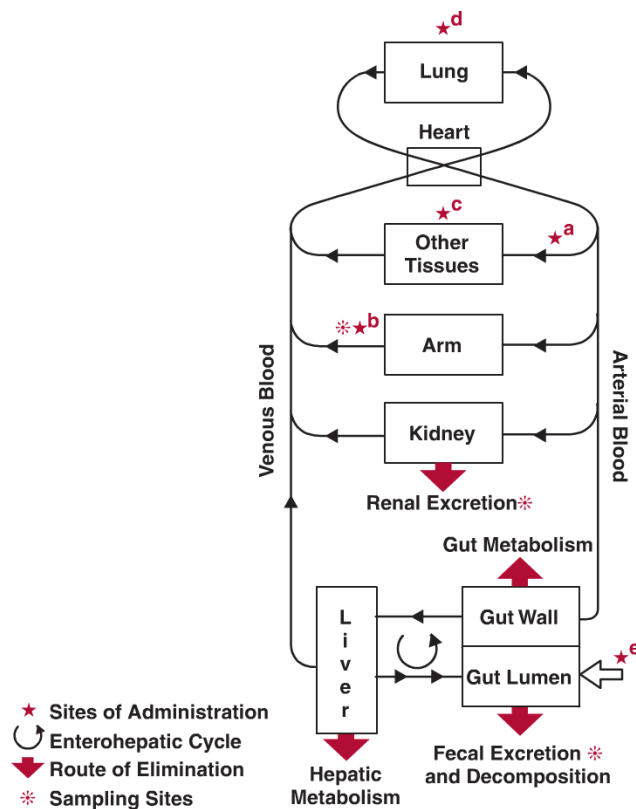


FIGURE 2-4. Once absorbed from any of the many sites of administration, drug is conveyed by blood to all sites within the body including the eliminating organs and site(s) of action. Sites of administration include: *a*, artery; *b*, peripheral vein; *c*, muscle and subcutaneous tissue; *d*, lung; and *e*, gastrointestinal tract, the open arrow. When given intravenously into an arm vein, the contralateral arm should then be used for sampling. The movement of virtually any drug can be traced from site of administration to site(s) of elimination.

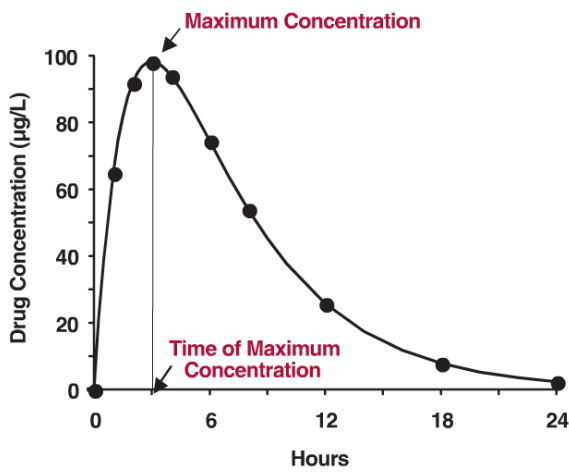


FIGURE 2-1. Drug concentration-time curve following a single oral dose showing the maximum systemic exposure (C_{max}) and the time of its occurrence (t_{max}). The concentration could represent drug in whole blood, plasma, or serum.

▪ ODE systems (differential equations)

- **Compartments:** organs
- **State variables:** drug & metabolite amounts
- **Rate rules:**
 - Blood flows, Transport, Disposition
 - Metabolism, Elimination
 - Absorption
- **Parameters:**
 - Tissue partition coefficients
 - Protein binding
 - Kinetic parameter (transport & elimination)
 - Blood flows, organ volumes, ...

▪ Result: Time dependent concentrations of substances/drugs in organs, blood & urine

- High pharmacological relevance since it enables the estimation of drug exposure not only in plasma but also at the site of action

ADME

Absorption, Distribution, Metabolism, Elimination

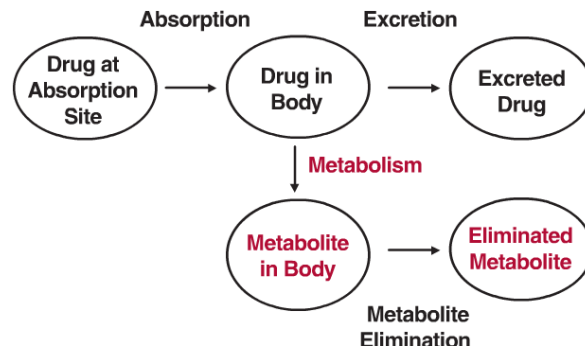
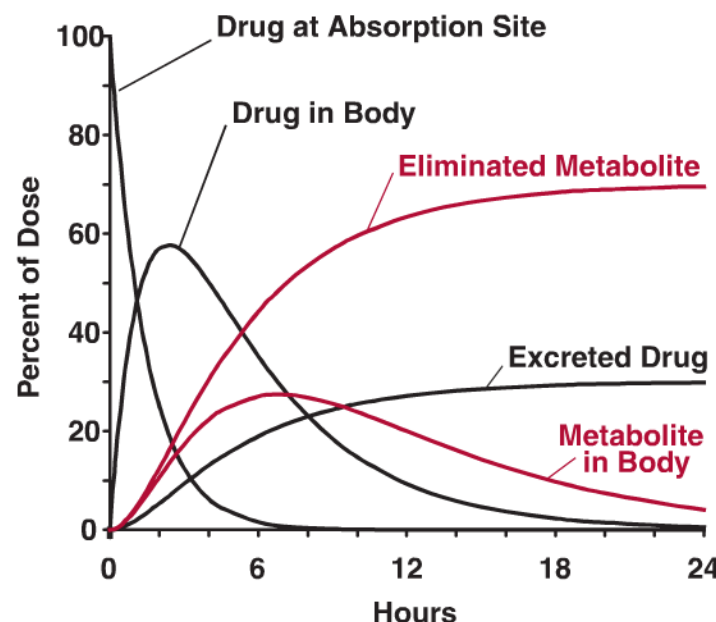


FIGURE 2-5. A drug is simultaneously absorbed into the body and eliminated from it, by excretion and metabolism. The processes of absorption, excretion, and metabolism are indicated with arrows and the compartments represent different locations and different chemical species (color = metabolite). Metabolite elimination may occur by further metabolism or excretion.

$$Dose = \frac{Amount\ at\ Absorption\ Site}{ } + \frac{Amount\ in\ Body}{ } + \frac{Amount\ Excreted}{ } + \frac{Amount\ Metabolized}{ } \quad 2-1$$

$$\text{Rate of Change of Drug in Body} = \frac{\text{Rate of Absorption}}{} - \left[\frac{\text{Rate of Excretion}}{} + \frac{\text{Rate of Metabolism}}{} \right] \quad 2-2$$

FIGURE 2-6. Time course of drug and metabolite in each of the compartments shown in Fig. 2-5. The amount in each compartment is expressed as a percentage of the dose administered. In this example, all the dose is absorbed. At any time, the sum of the molar amounts in the five compartments equals the dose.



Analysis

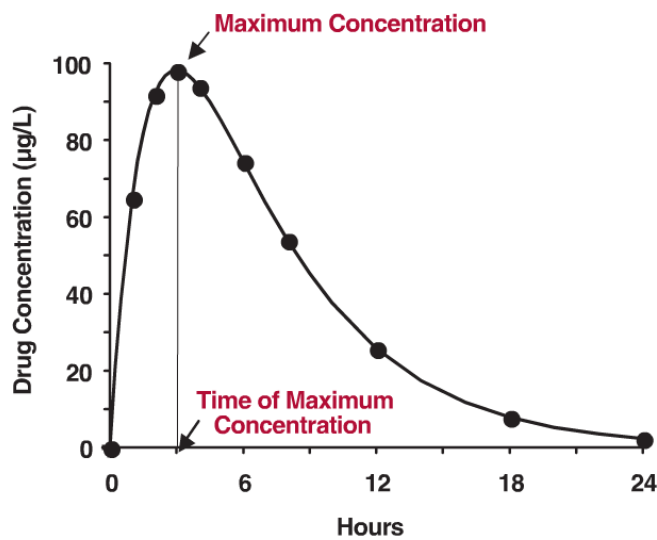


FIGURE 2-1. Drug concentration-time curve following a single oral dose showing the maximum systemic exposure (C_{max}) and the time of its occurrence (t_{max}). The concentration could represent drug in whole blood, plasma, or serum.

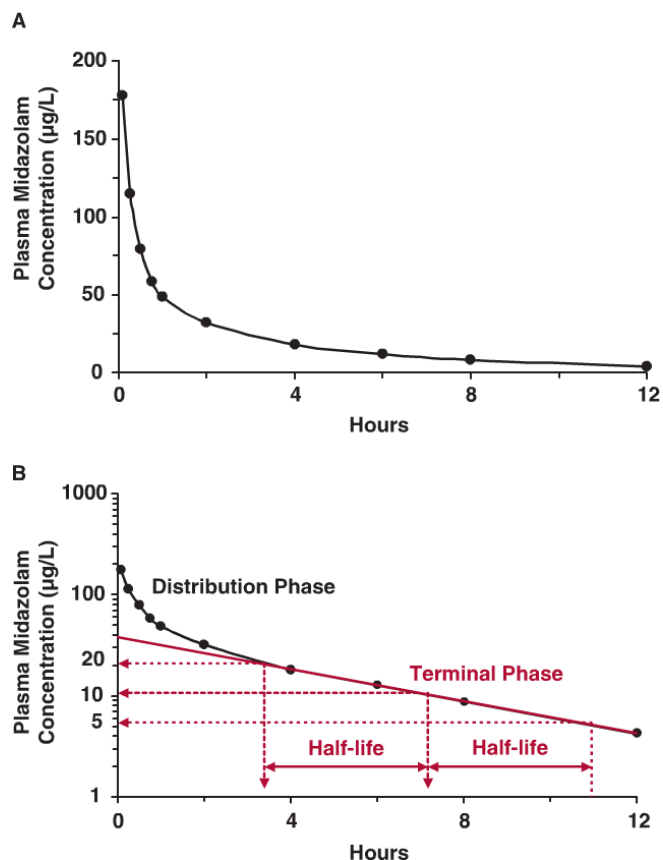


FIGURE 3-4. A. Plasma concentration of midazolam with time in an individual after an 8.35-mg i.v. bolus dose of midazolam hydrochloride (7.5 mg of the base) in a healthy adult. B. The data in A are redisplayed as a semilogarithmic plot. Note the short distribution phase. (From: Pentikäinen PJ, Välijoki L, Himberg JJ, Crevoisier C. Pharmacokinetics of midazolam following i.v. and oral administration in patients with chronic liver disease and in healthy subjects. *J Clin Pharmacol* 1989;29: 272–277.)

- C_{max} : Maximal concentration
- T_{max} : time of maximal concentration
- **AUC**: area under the curve
- k_{el} : elimination rate fitting linear part of terminal phase (log)
- $t_{1/2}$: half-life ($= \ln 2/k_{el}$) time for concentration to fall to half
- V_d : volume of distribution ($= CL/k$), dilution space
- CL : clearance ($= \text{Dose}/\text{AUC}$, $= \text{Dose}/C(0)_{\text{extrapolated}}$)

- Every substance is different (ADME), physiology stays the same

Kuepfer2016

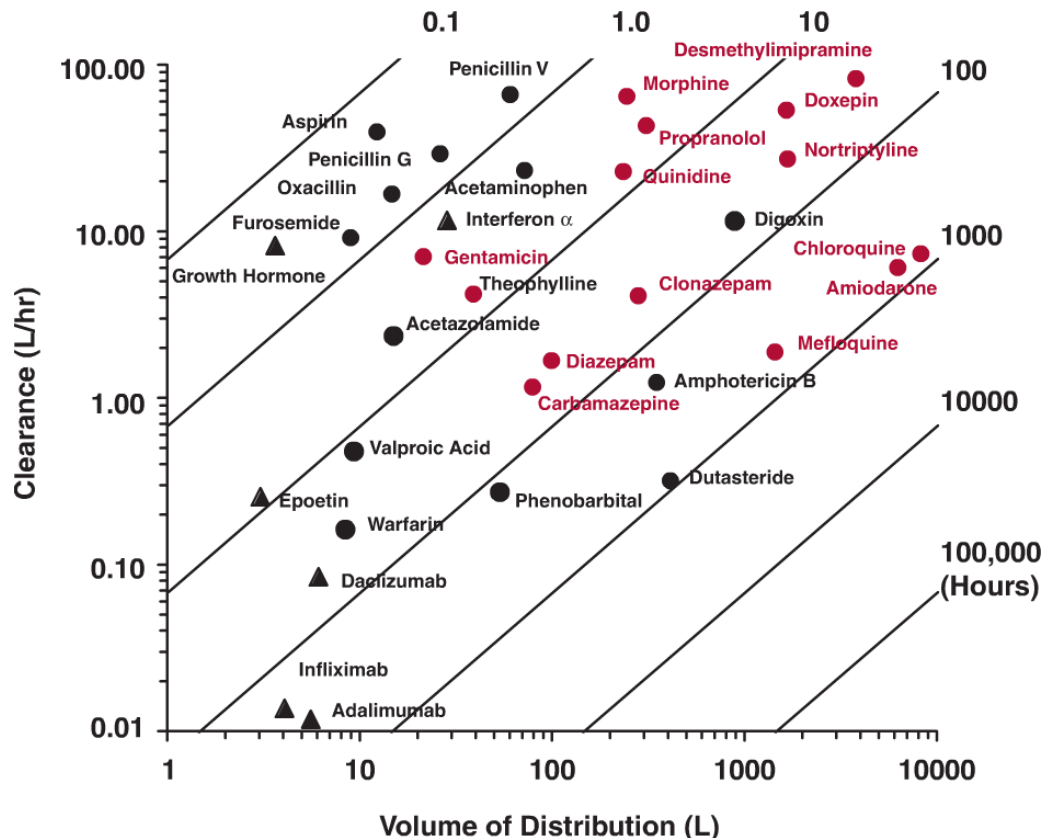
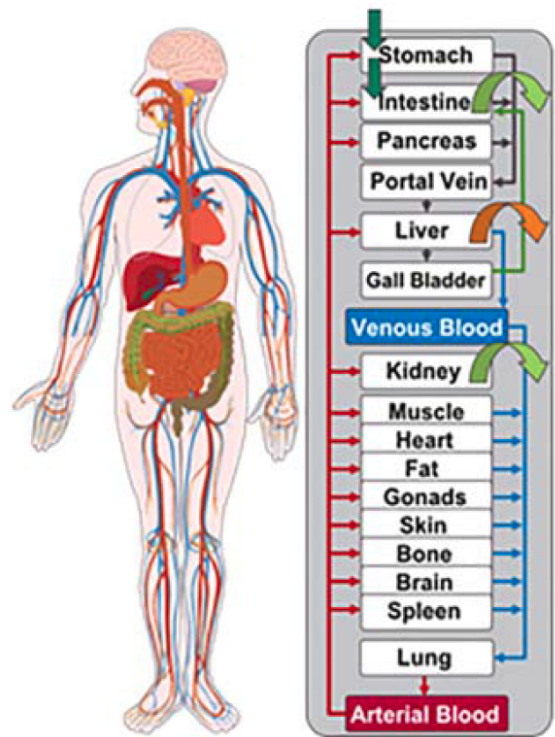


FIGURE 5-18. Clearance (ordinate) and volume of distribution (abscissa) of selected acidic (●, digoxin is neutral) and basic (●), as well as protein (▲), drugs varies widely. The diagonal lines show the combination of clearance and volume with the same half-lives (in hours). Note that drugs with very low clearance and very large volumes (lower right-hand quadrant of graph) are uncommon; their half-lives are often too long for these drugs to be used practically in drug therapy. Note also that protein drugs have volumes of distribution close to plasma volume, and that basic compounds tend to have larger volumes of distribution than acids. Digoxin is a neutral compound, whereas amphotericin B is both an acid and a base.

Rowland2011

Large individual variability

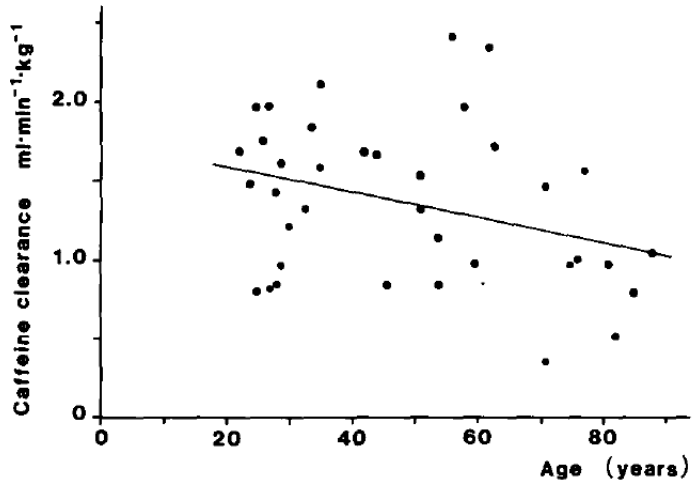


Fig. 2. Caffeine saliva clearance in healthy normal subjects as a function of age. The systemic clearance of caffeine decreases significantly with age ($P < 0.05$).

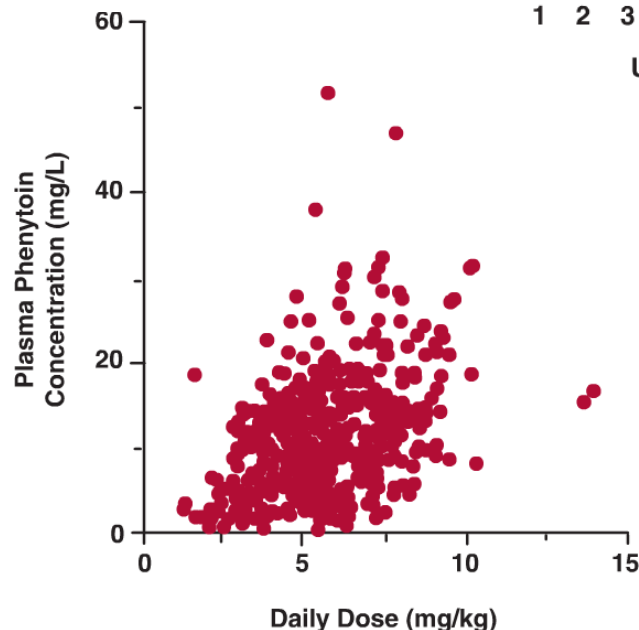
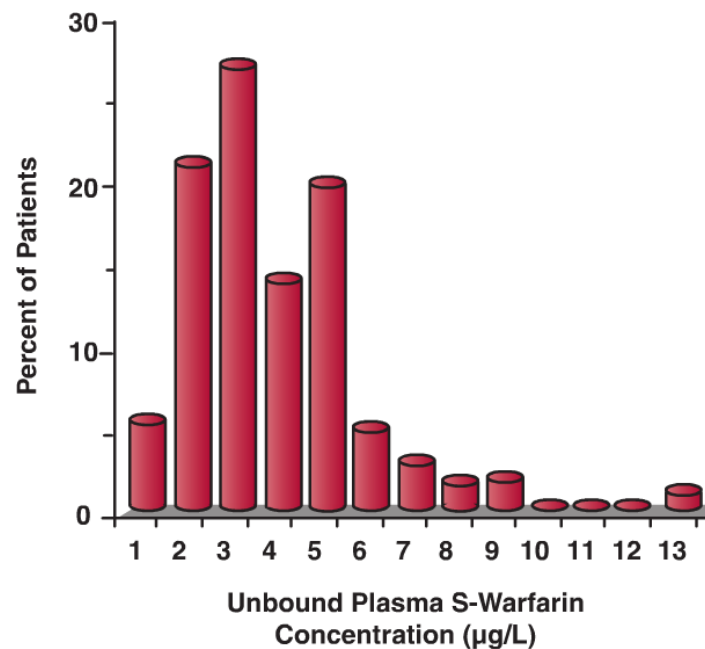


FIGURE 1-7. Although the average plasma concentration of phenytoin on chronic dosing tends to increase with the dosing rate, there is large variation in the individual values. (From: Lund, L. Effects of phenytoin in patients with epilepsy in relation to its concentration in plasma. In Davies DS, Prichard BNC, eds. Biological Effects of Drugs in Relation to Their Plasma Concentration. London and Basingstoke: Macmillan, 1973:227–238.)

FIGURE 1-8. There is considerable interindividual pharmacodynamic variability in response to the oral anticoagulant warfarin as demonstrated by the substantial spread in the unbound concentration of the active S-isomer associated with a similar degree of anticoagulation in a group of 97 patients on maintenance therapy. (From: Scordo MG, Pengo V, Spina E, et al. Influence of CYP2C9 and CYP2C19 genetic polymorphisms of warfarin maintenance dose and metabolic clearance. Clin Pharmacol Ther 2002;72:702–710.)

Variability Liver Enzymes

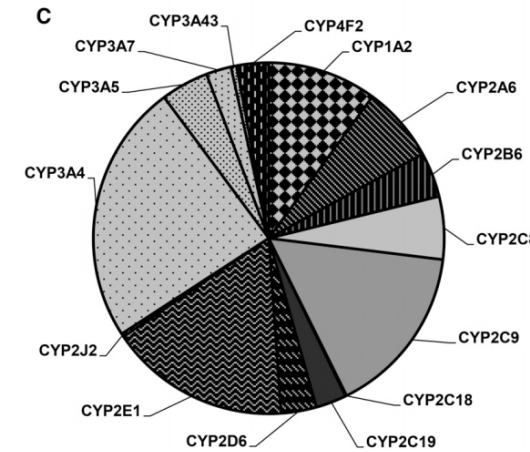
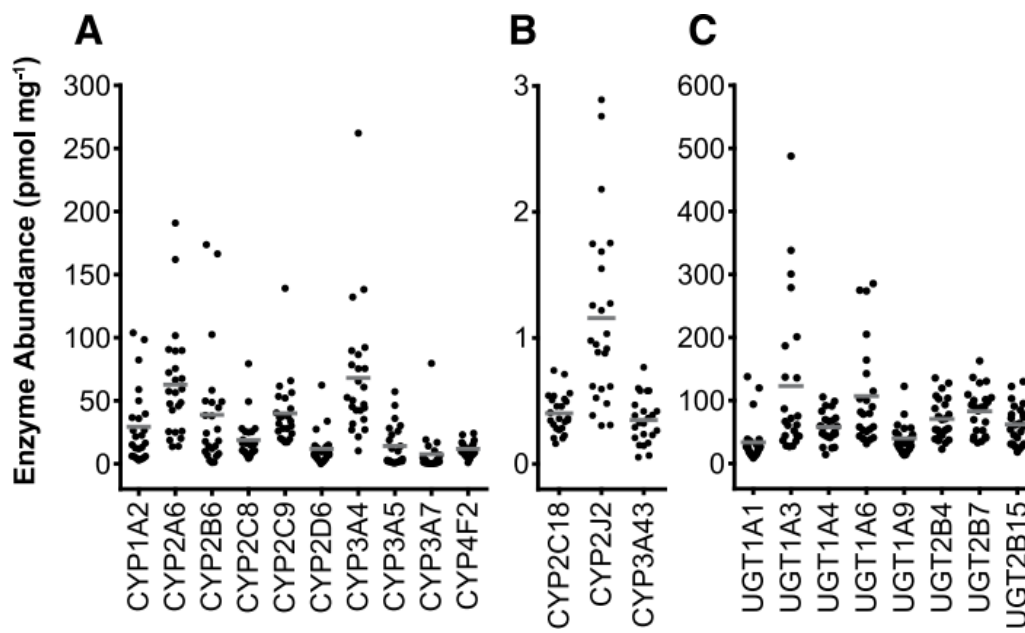


Fig. 1. Bar graph (A and B) and pie chart (C) of weighted mean abundances of cytochrome P450 enzymes in livers from adult Caucasians. Error bars represent weighted standard deviation values. n , the number of livers.



Archour2014b

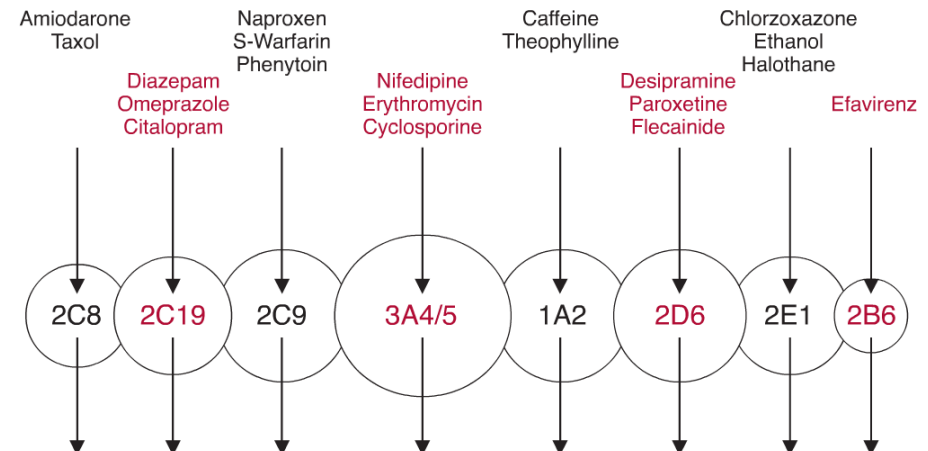


FIGURE 5-3. Graphic representation of the different forms of human cytochrome-P450 enzyme (circles) with different but often overlapping substrate specificities. The arrows indicate the single metabolic pathways. Representative substrates are listed above each enzyme.

Fig. 2. A scatter plot of the measured abundance values of P450 (A and B) and UGT (C) enzymes. The number of samples is 24 for each enzyme except CYP2C9, CYP3A5, CYP3A7, CYP3A43, UGT1A3, UGT1A4, and UGT1A6 ($n = 23$). Lines indicate population means of the sets of data.

Pharmacogenomics

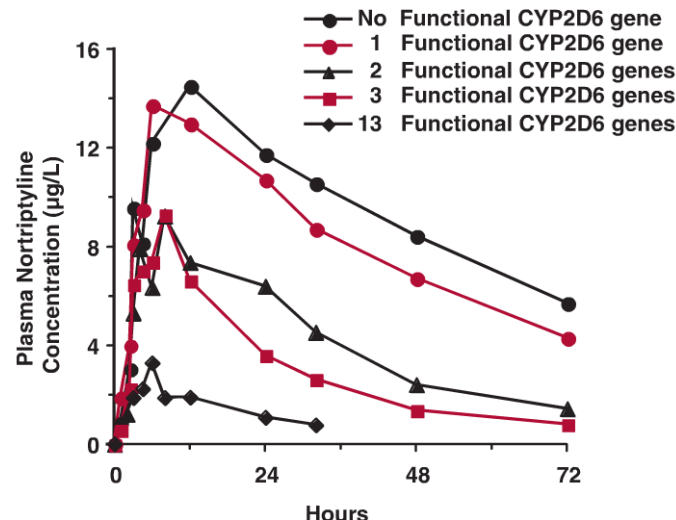


FIGURE 13-2. Strong genetic influence in the pharmacokinetics of nortriptyline is clearly demonstrated by the high correlation between the plasma concentration–time profile and the number of functional CYP2D6 genes possessed by an individual; the larger the number of functional genes, the higher is the clearance and the lower is the exposure profile following a single 25-mg dose of nortriptyline. (From: Dalén P, Dahl ML, Bernal Ruiz ML, et al. 10-Hydroxylation of nortriptyline in white persons with 0, 1, 2, 3, and 13 functional CYP2D6 genes. Clin Pharmacol Ther 1998;63:444–452.)

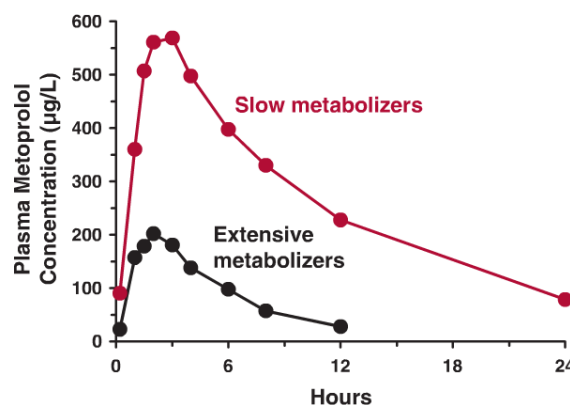


FIGURE 13-3. Plasma metoprolol concentrations after a single oral dose of 200-mg metoprolol tartrate were much higher in poor (colored line) than in extensive (black line) CYP2D6 metabolizers. Because metoprolol is a drug of high hepatic clearance, the difference between poor and extensive metabolizers is expressed in the large difference in oral bioavailability, because of differences in first-pass hepatic loss. (From: Lennard MS, Silas JH, Freestone S, et al. Oxidative phenotype—a major determinant of metoprolol metabolism and response. Reprinted by permission of New Eng J Med 1982;307:1558–1560.)

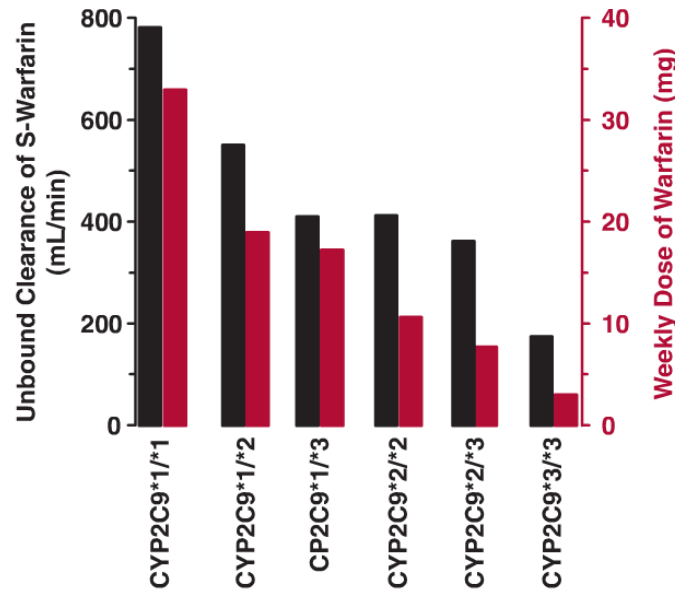
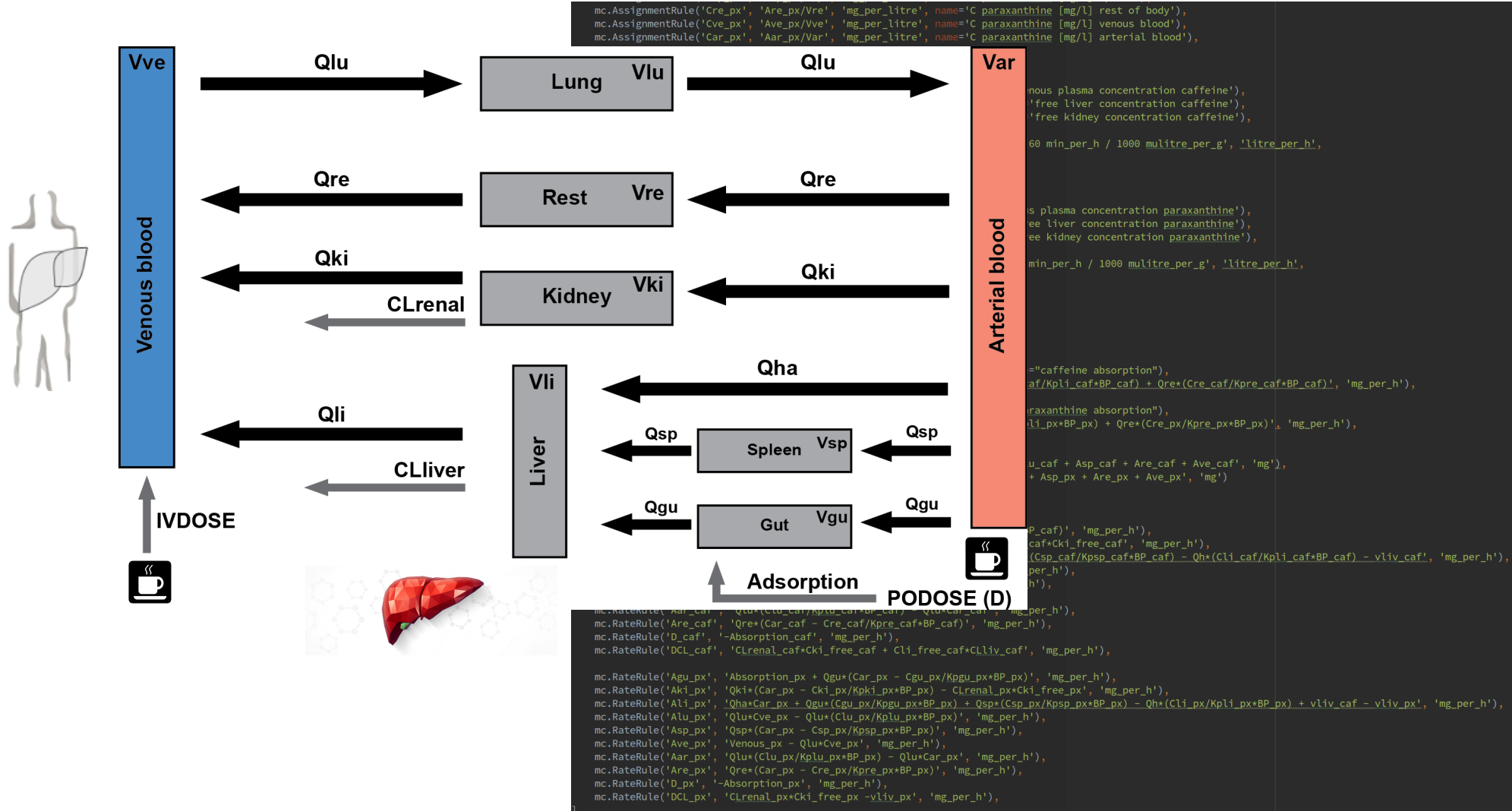


FIGURE 13-4. Genetics plays a significant role in the maintenance dose requirement of warfarin used in the treatment of various cardiovascular diseases. Shown are the unbound clearance of S-warfarin (black) in groups of patients with different CYP2C9 genotypes, all titrated and stabilized to a narrow target INR (International Normalization Ratio) range, a measure of anticoagulation, of between 2 and 3, and the mean weekly maintenance dose (obtained by summing the daily dose over 1 week, in color). Warfarin is administered as the racemate, with most of the therapeutic effect associated with the more active S-isomer, which is primarily eliminated by CYP2C9-catalyzed metabolism. Homozygous patients with two wild-type alleles (denoted by CYP2C9*1/*1) have the highest S-warfarin clearance and require the highest maintenance dose, and those with two of the most deficient alleles (CYP2C9*3/*3) have the lowest clearance and need the smallest maintenance dose. Heterozygous patients have intermediate clearance. However, as noted in Fig. 12-4 (Chapter 12, Variability), in addition to pharmacokinetic variability, there is also considerable interindividual variability in pharmacodynamics of this compound. (From: Scordo MG, Pengo V, Spina E, et al. Influence of CYP2C9 and CYP2C19 genetic polymorphisms of warfarin maintenance dose and metabolic clearance. Clin Pharmacol Ther 2002;72:702–710.)

Example: Caffeine



Example: Glucose-Insulin system

DallaMan2006, talk

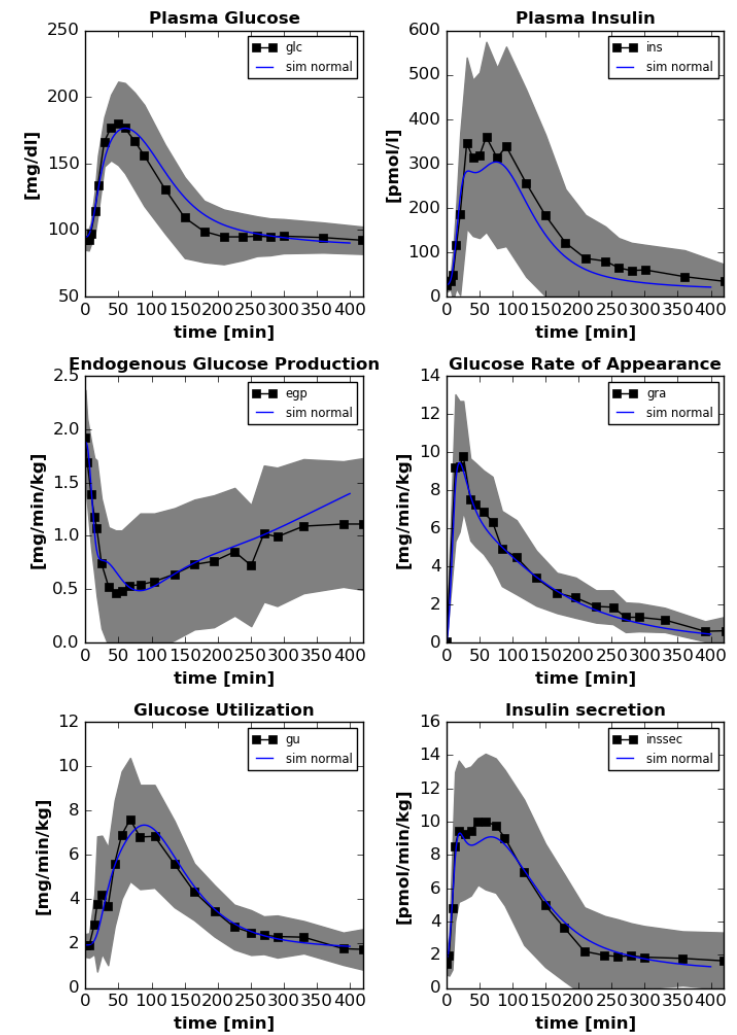
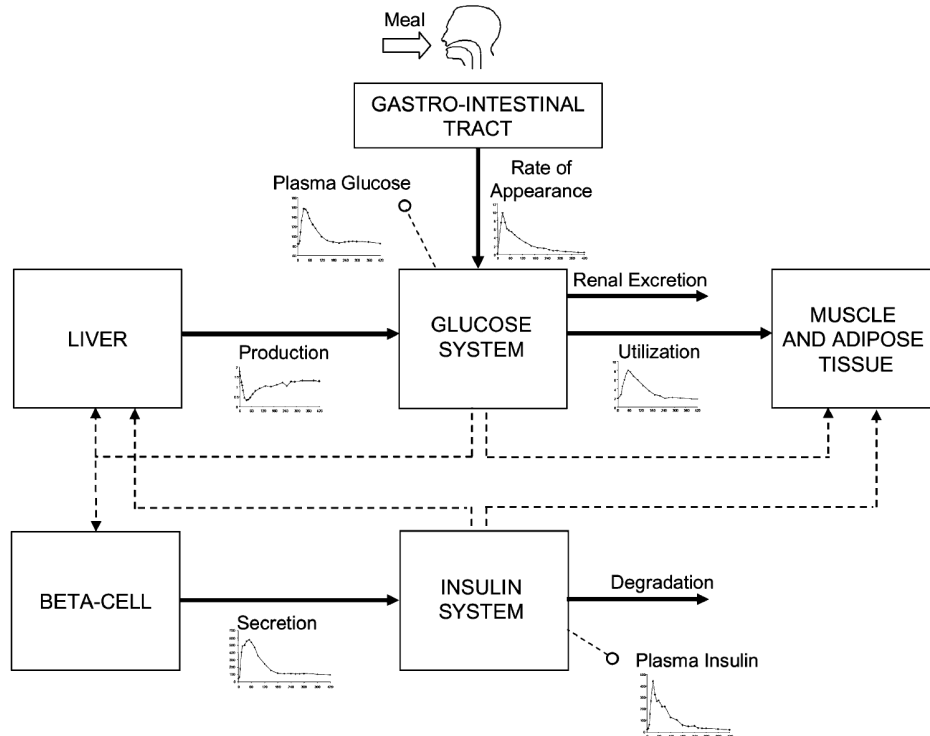


Fig. 2. Scheme of the glucose-insulin control system which puts in relation the measured plasma concentrations, i.e., glucose G , and insulin I , to glucose fluxes, i.e., rate of appearance R_a , production EGP , utilization U , renal extraction E , and insulin fluxes, i.e., secretion S , and degradation D .

Caffeine PKPD



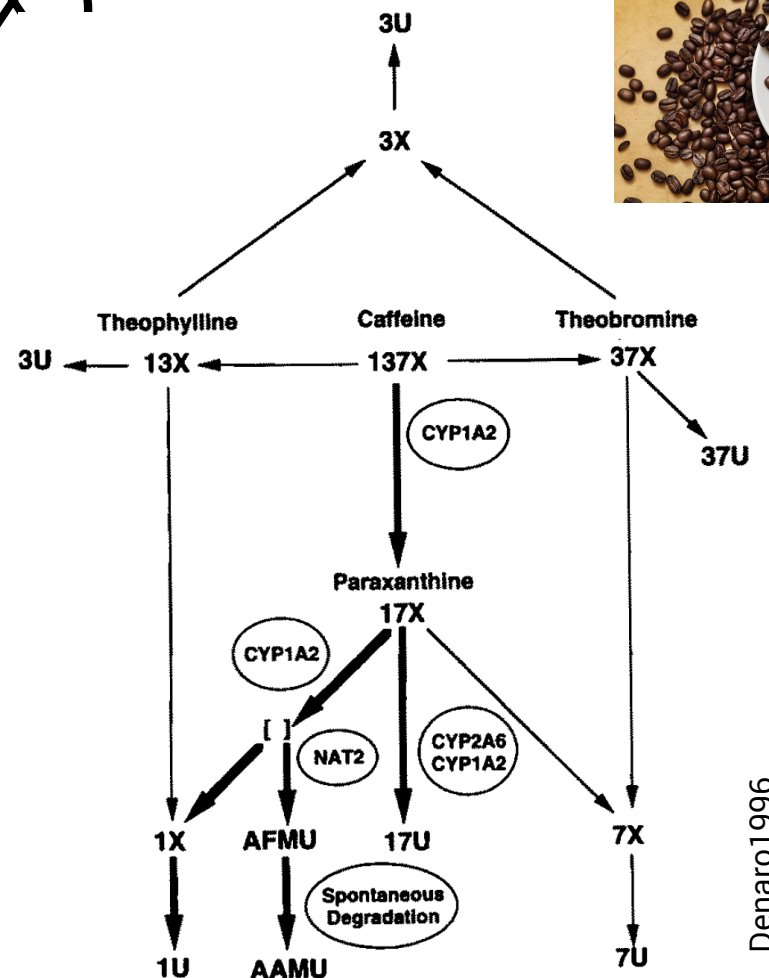
Caffeine & smoking



M. König, manuscript in preparation

Caffeine (137X)

- world's most widely consumed psychoactive drug
- Metabolized in liver by **CYP1A2**
 - to **paraxanthine (17X)**, theobromine & theophylline
- Classical liver function test
 - Time course of caffeine
 - urinary ratios of methyl-xanthines
 - Caffeine/paraxanthine ratio
- Large Variability
 - Effects of lifestyle on expression
 - Smoking is one of such lifestyle factors



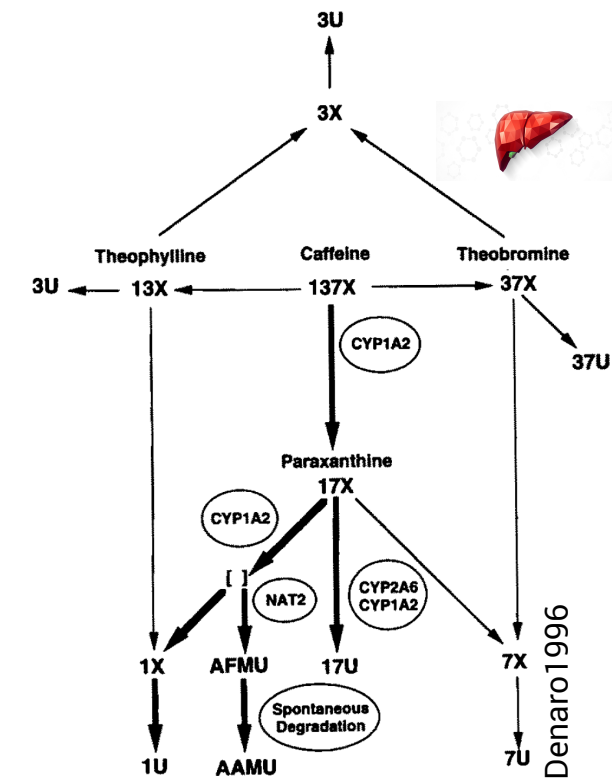
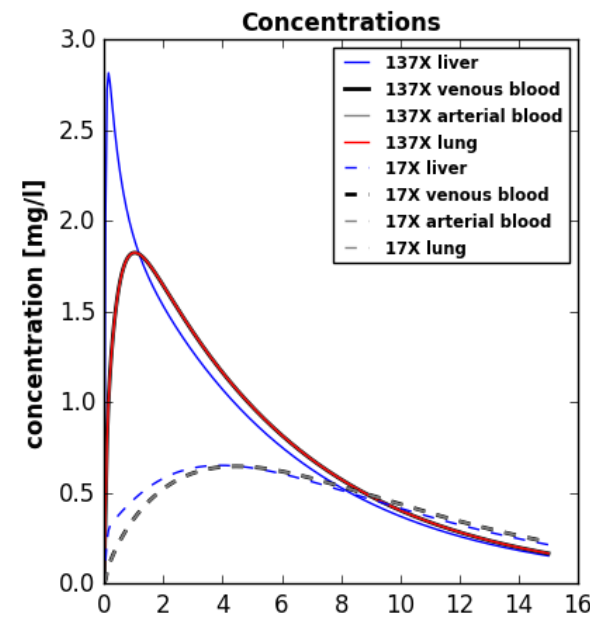
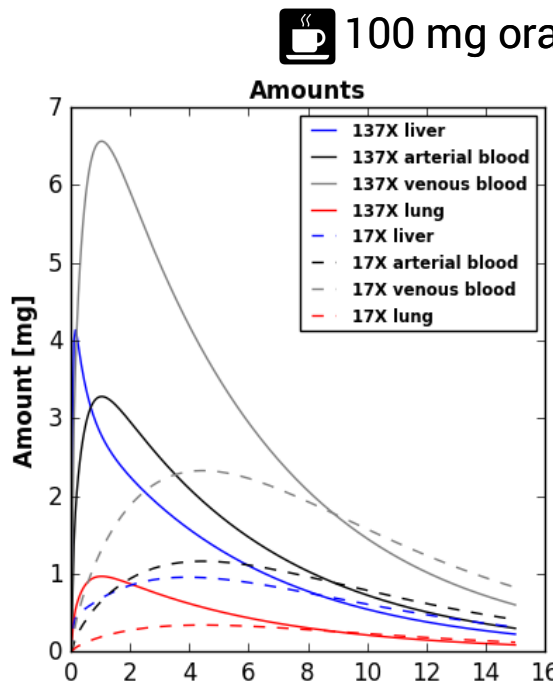
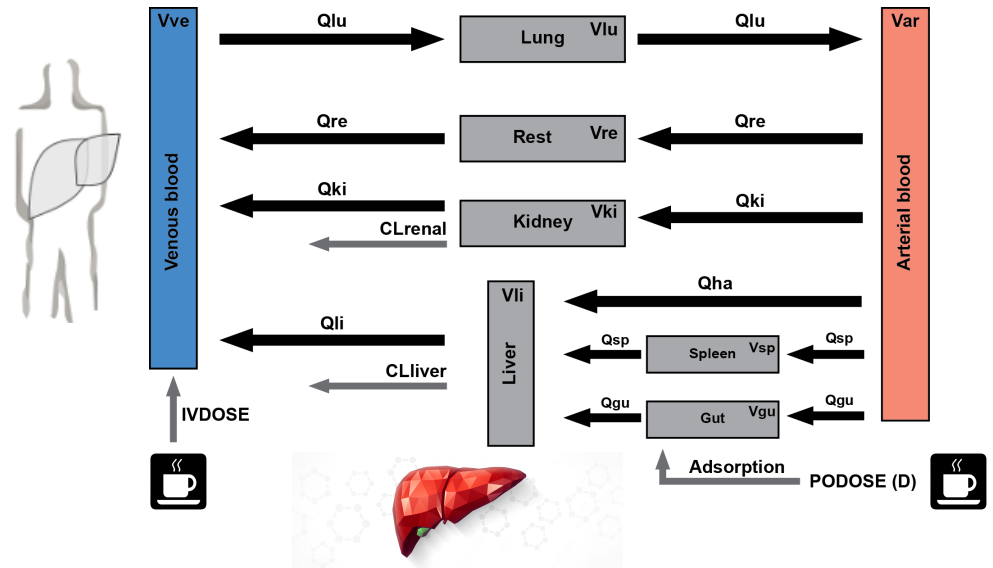
Denaro1996

- How is smoking affecting the clearance of caffeine ?

$$\text{Cup of Coffee} + \text{Smoking} = ?$$

PKPD

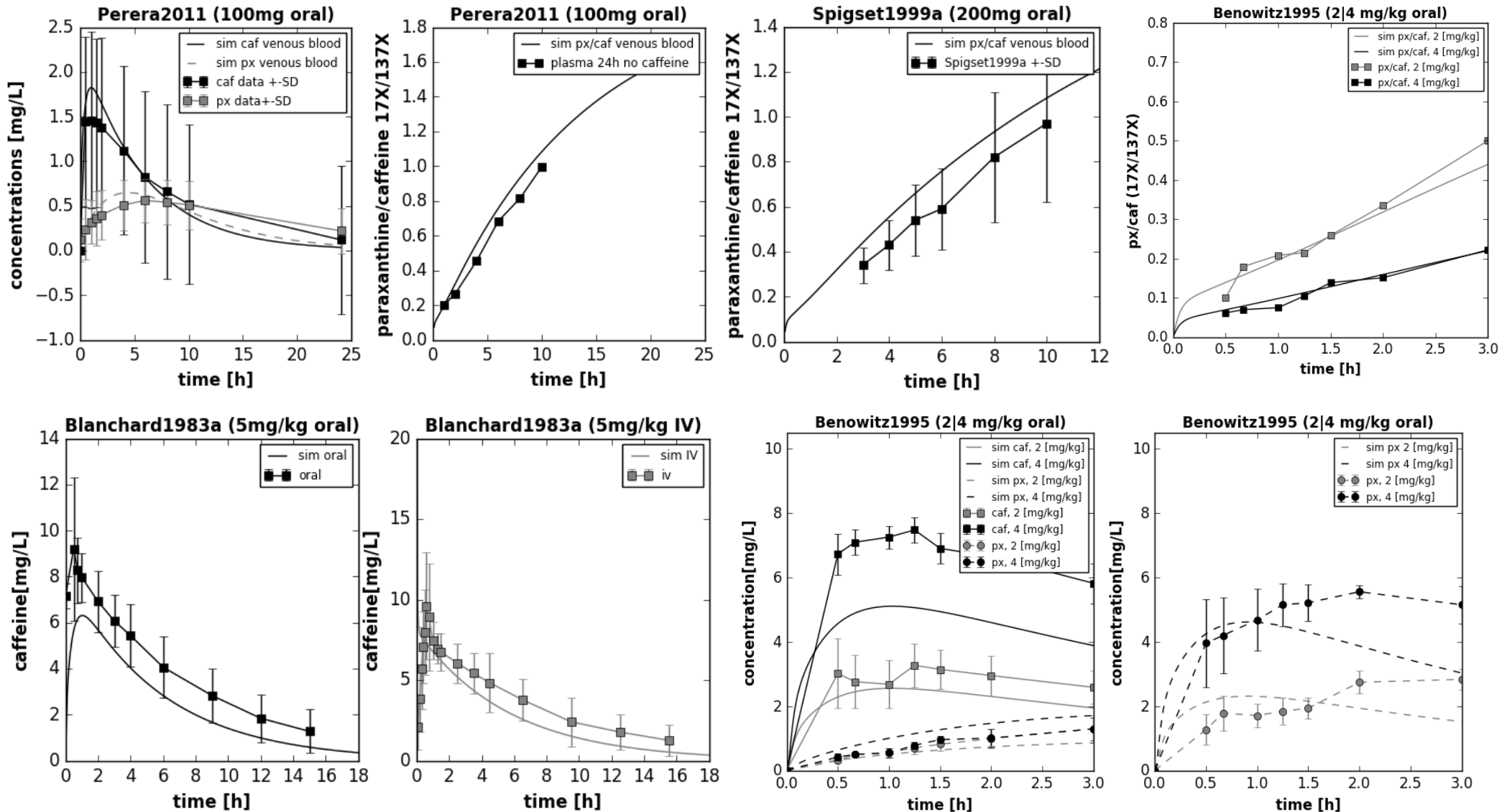
- Kinetic model of caffeine liver metabolism
- Renal clearance
- Whole-body distribution kinetics



Mean model



human (70kg, male),
mean microsomal CYP1A2 content,
non-smoker

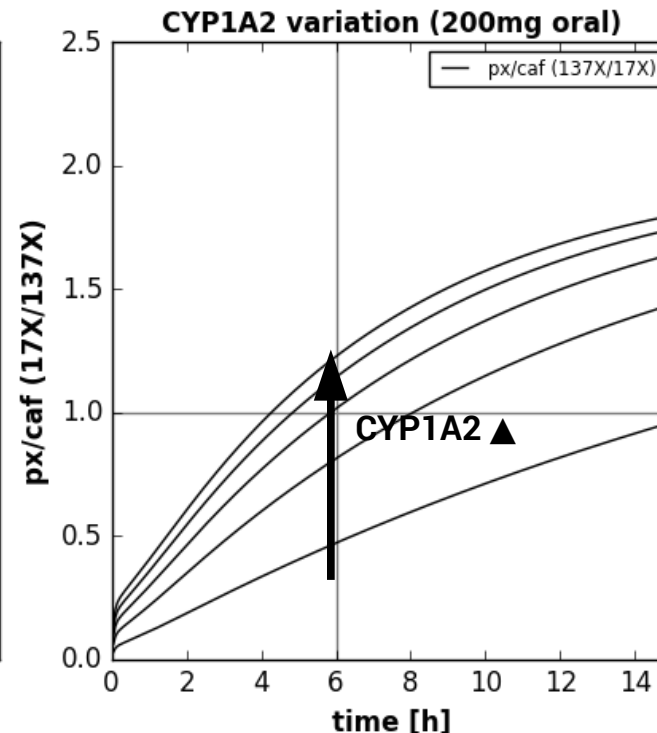
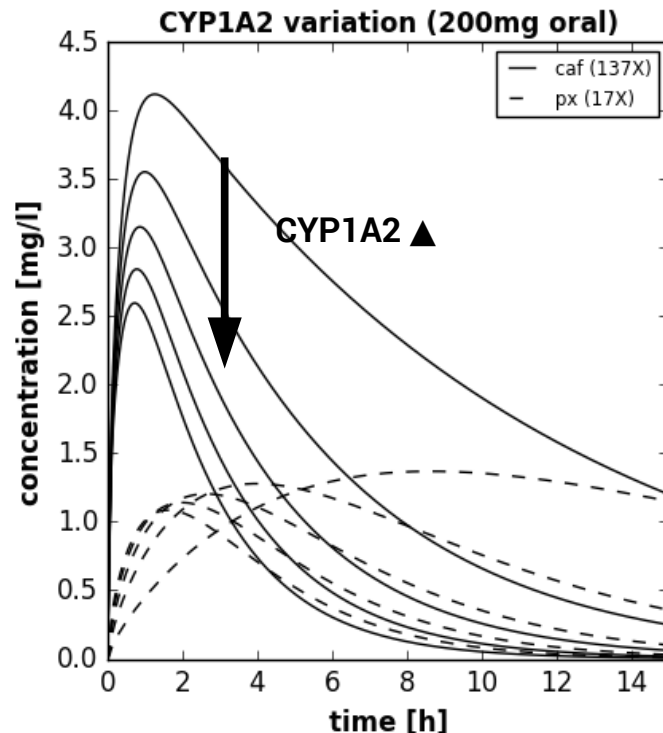


CYP1A2

- CYP1A2 expression altered by many lifestyle factors
 - Strong effect: **Smoking**
- Altered function test results
 - clearance, half-life, kel, max value, metabolic ratios

Table 4. Parameter estimates of covariates obtained for logarithmic clearance values using the paraxanthine/caffeine ratio method (equation 1)

Covariate	Symbol used in equation 5	Estimate	95% Confidence interval		Mean resulting change of clearance (factor)
			Lower bound	Upper bound	
-	Intercept	0.264	-0.015	0.542	-
Coffee intake (litre day ⁻¹)	Slope _{coffee}	0.368	0.287	0.449	1.445
Body mass index (kg m ⁻²)	Slope _{BMI}	-0.010	-0.018	-0.002	0.990
Cigarettes/day					
Non-smokers	$V_{\text{smoking habit index}}$	0	-	-	Reference
1–5		0.195	0.065	0.324	1.215
6–10		0.383	0.253	0.509	1.467
11–20		0.504	0.386	0.621	1.655
>20		0.543	0.430	0.655	1.721
Oral contraceptives					
No	$V_{\text{oral contraceptive index}}$	0	-	-	Reference
Yes		-0.332	-0.236	-0.428	0.717
Country					
Germany	$V_{\text{country of residence index}}$	0	-	-	Reference
Bulgaria		-0.209	-0.356	-0.061	0.811
Slovakia		-0.303	-0.450	-0.156	0.739
Sex					
Male	$V_{\text{sex index}}$	0	-	-	Reference
Female		-0.111	-0.178	-0.044	0.895



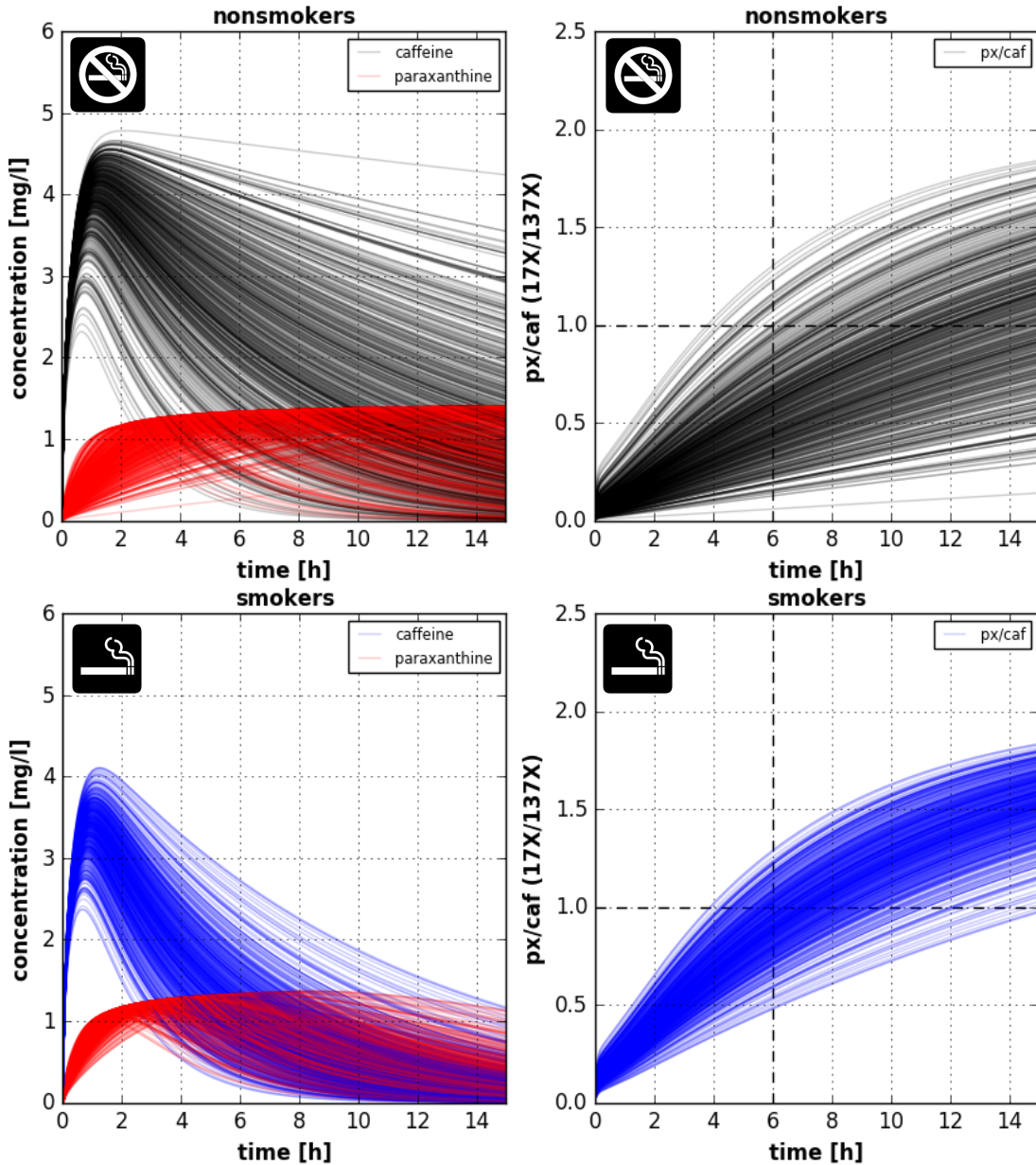
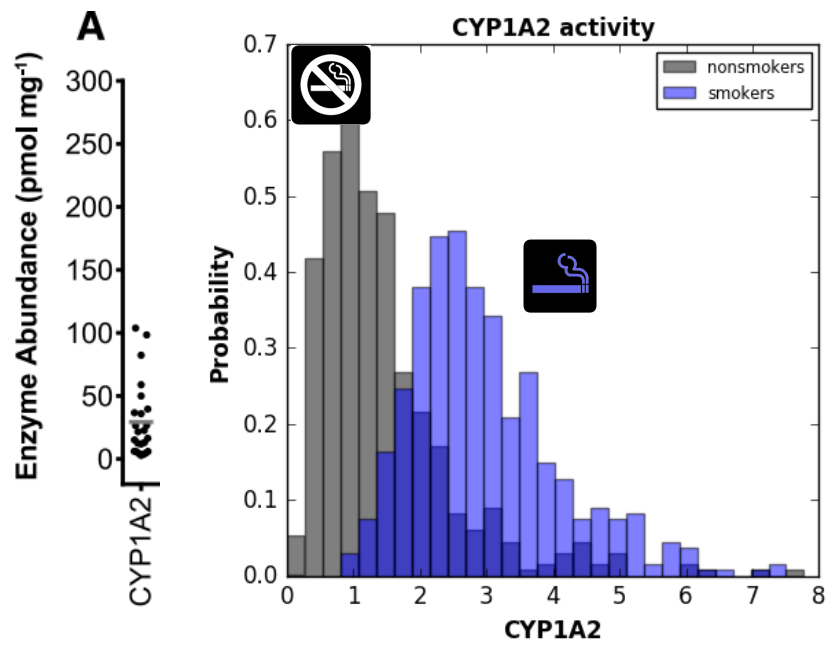
CYP1A2 induction ▲

- Clearance ▲
- kel ▲
- T_{1/2} ▼
- T_{max} ▼
- px(17X)/caf(137X) ▲

Smoking

- CYP1A2 smoking effect

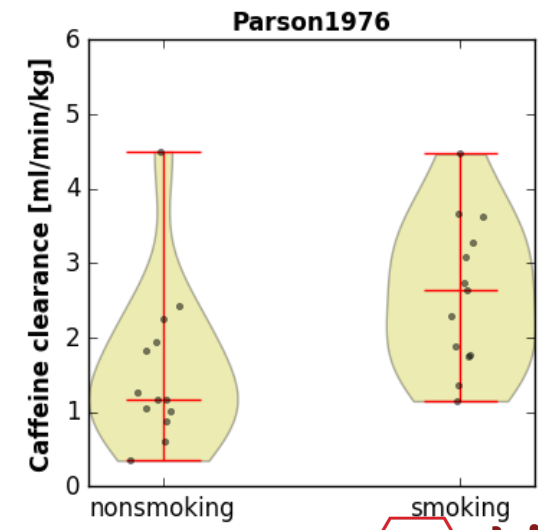
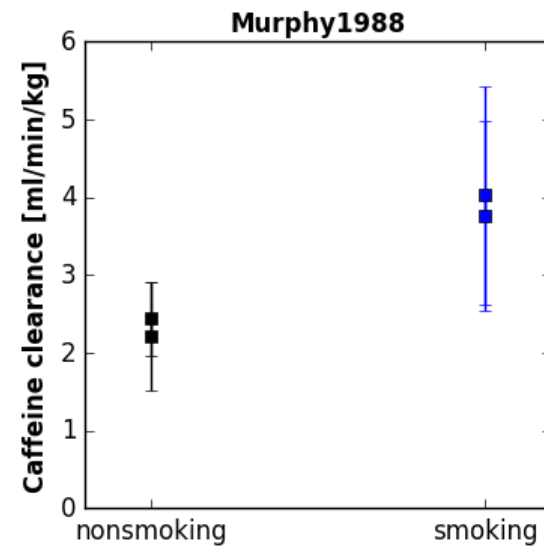
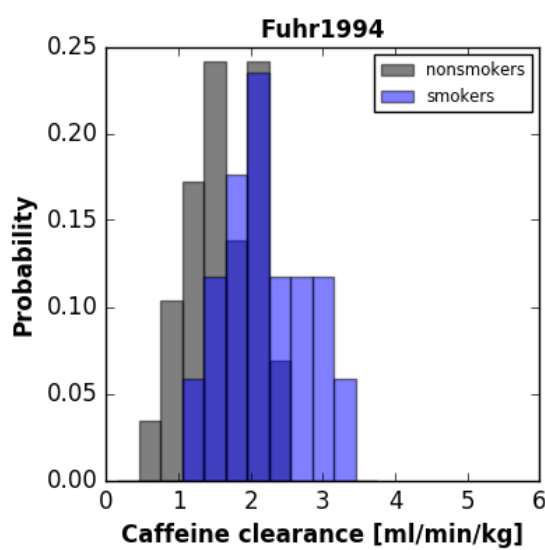
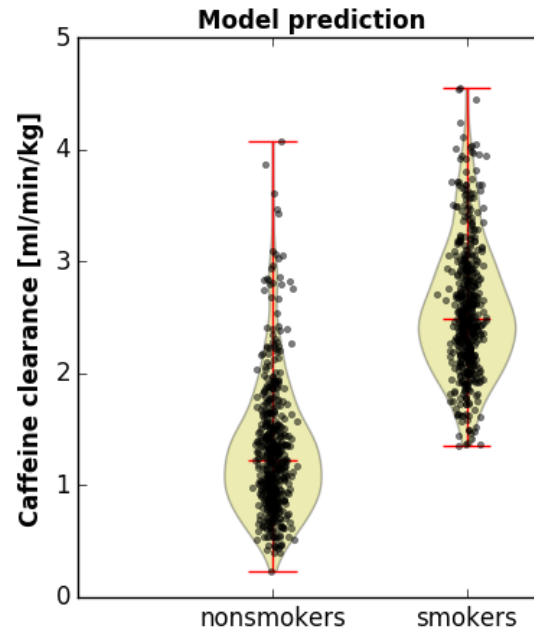
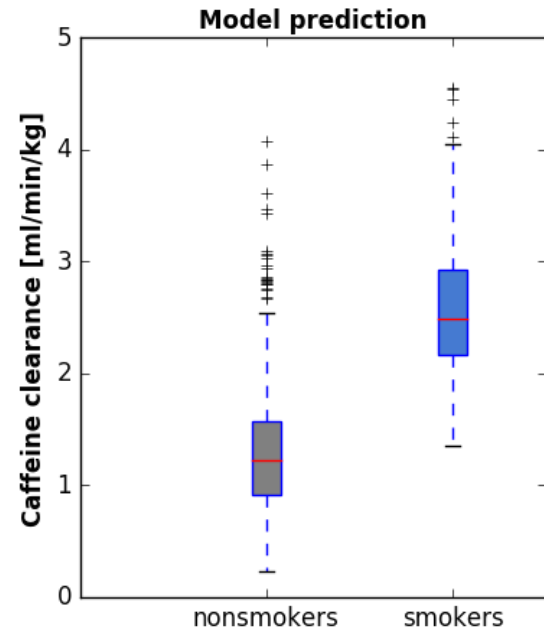
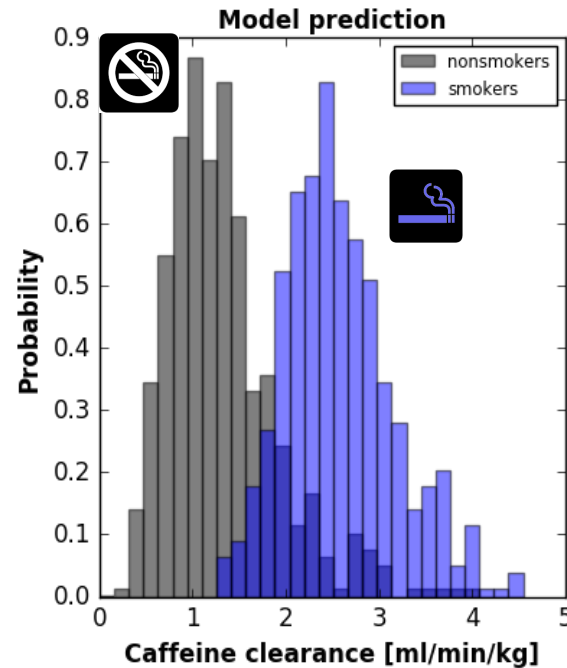
- Distribution of liver microsome activity (log-normal) for non-smokers and smokers
- Simulation of moderate smoking effect (6-10 cigarettes, ~40% increase)



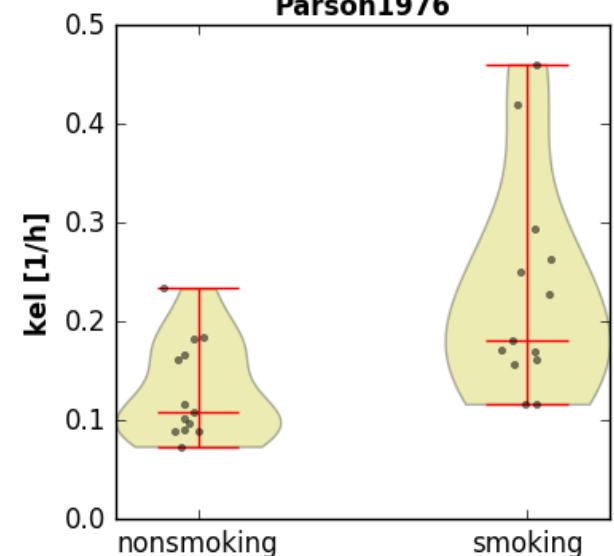
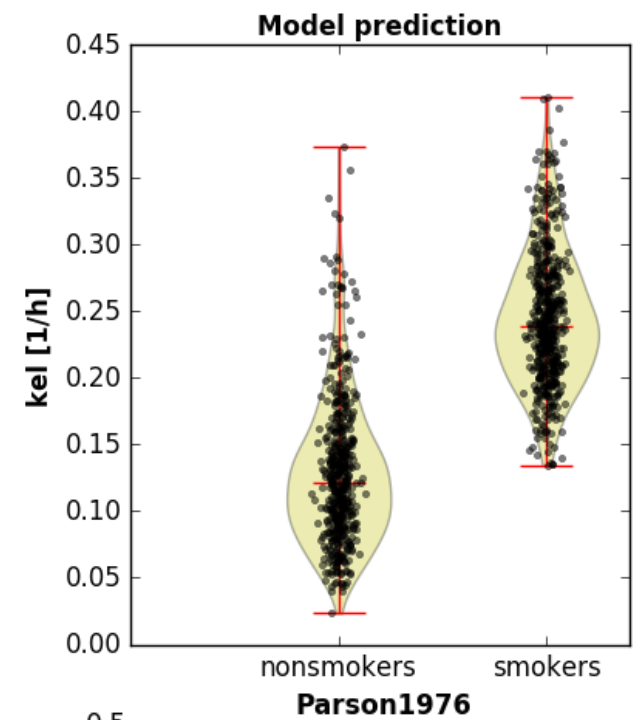
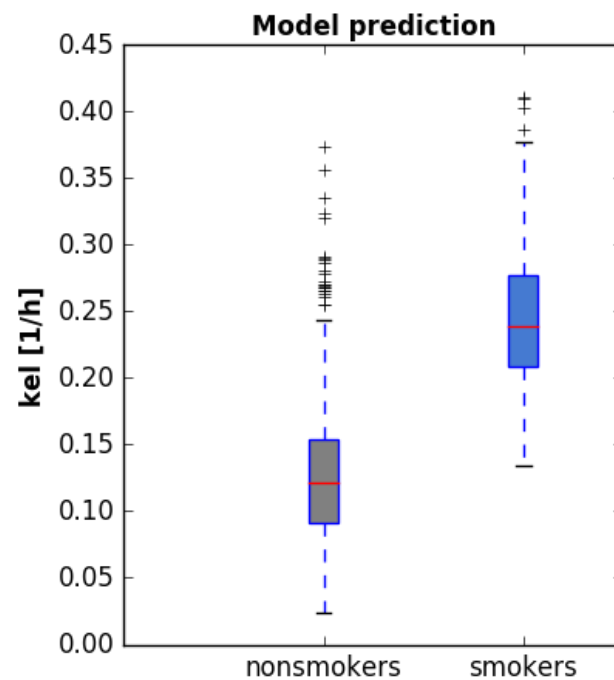
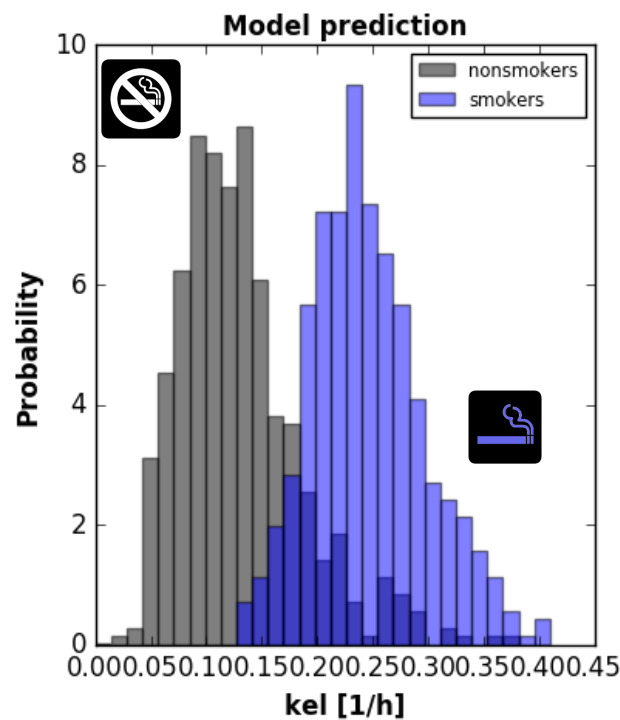
The weighted means, coefficients of variation (CV), ranges, and heterogeneity analysis of the analyzed hepatic cytochrome P450 enzyme abundance data from 50 studies

Enzyme	Mean	CV (%)	Range*	No. of Livers	Q	I^2	Heterogeneity	Studies ^a
CYP1A2	39 pmol mg^{-1}	78 %	1–263	148	19.54	54 %	Medium	[1–10]

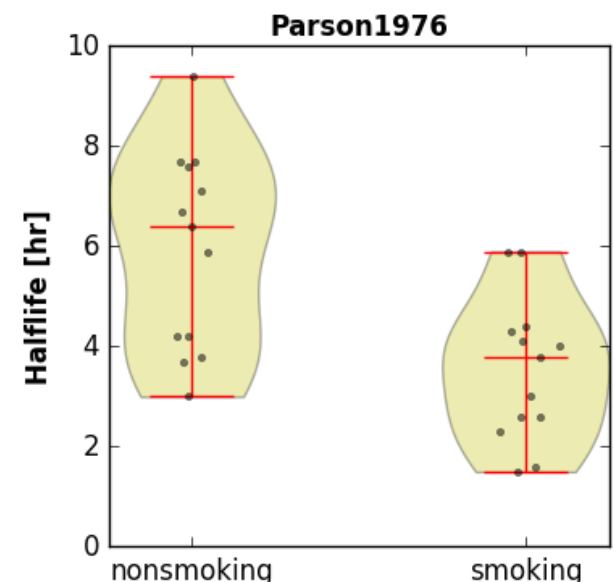
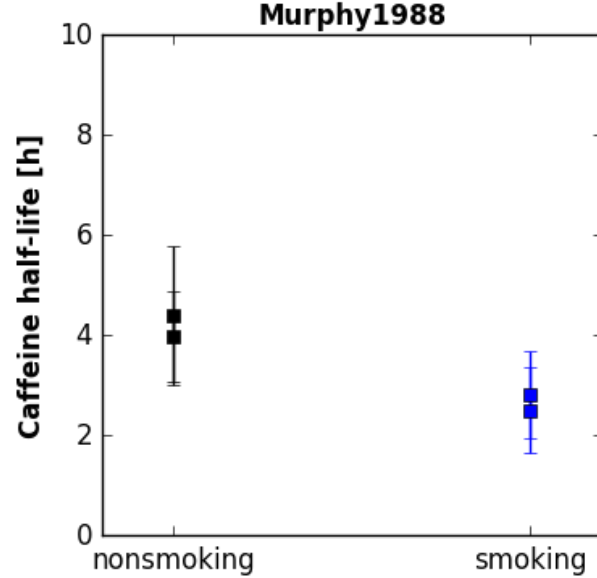
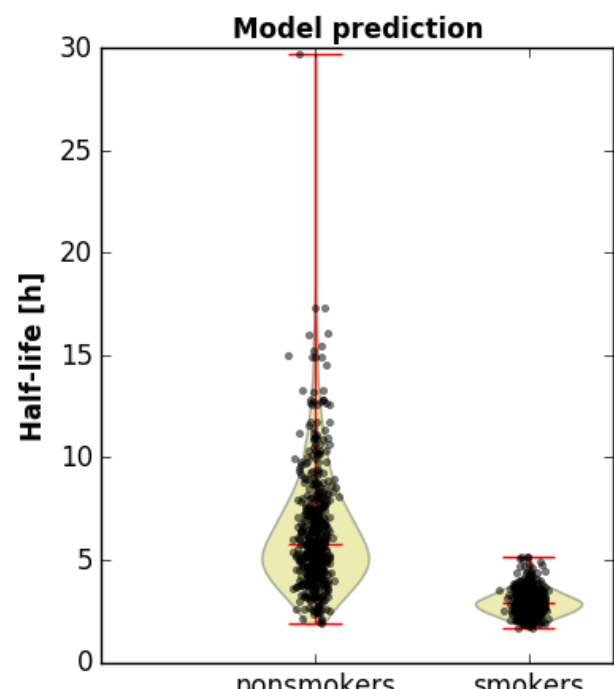
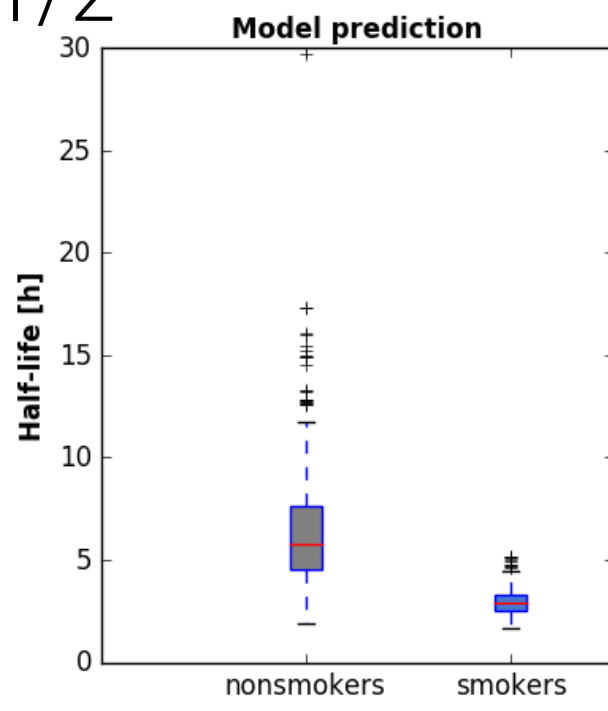
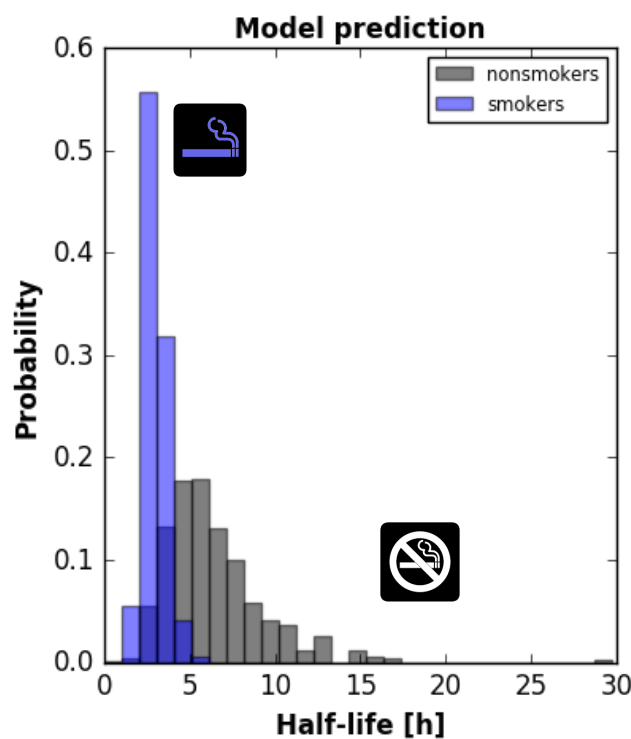
CL: Clearance



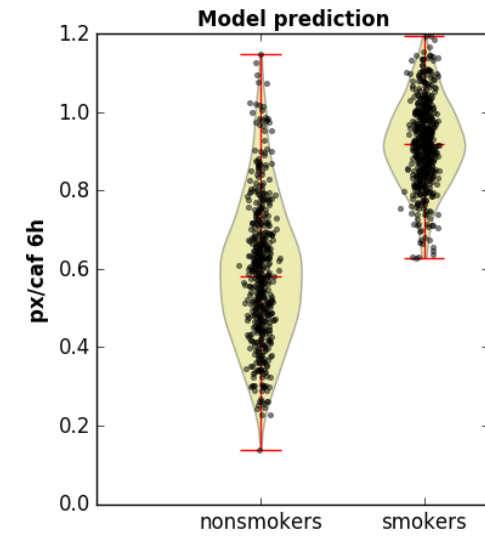
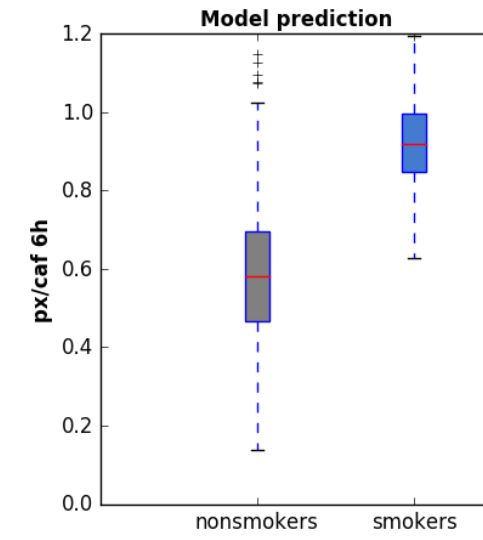
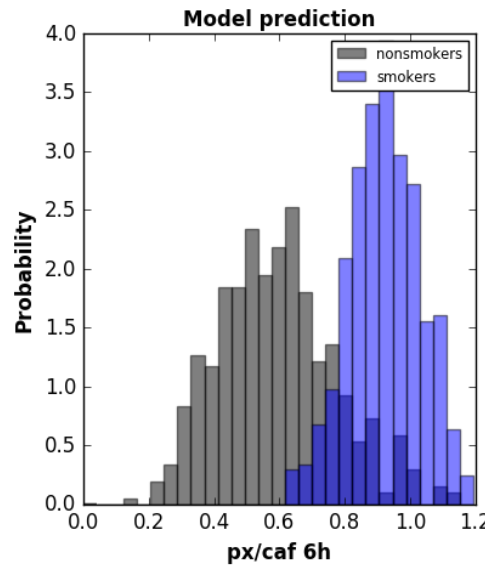
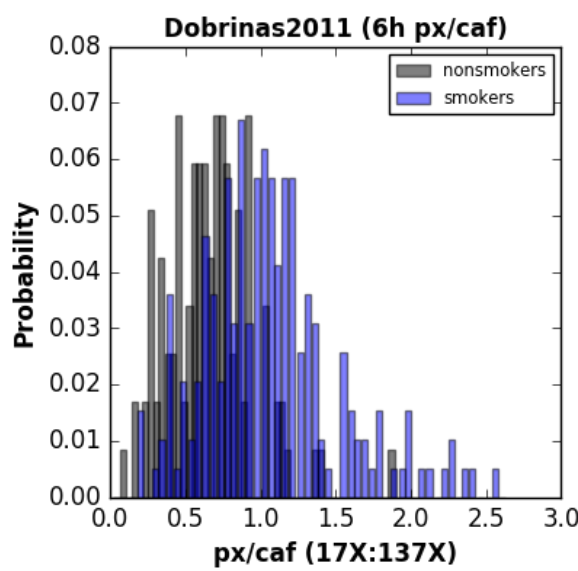
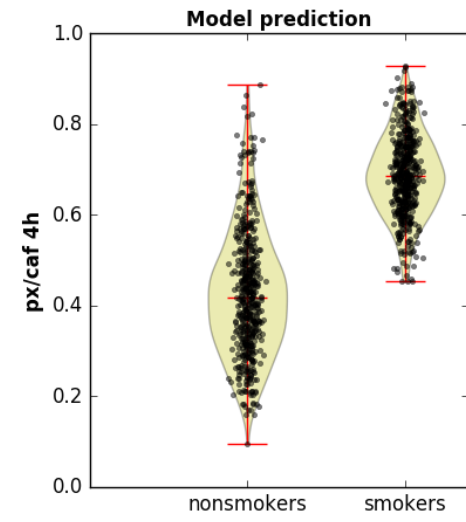
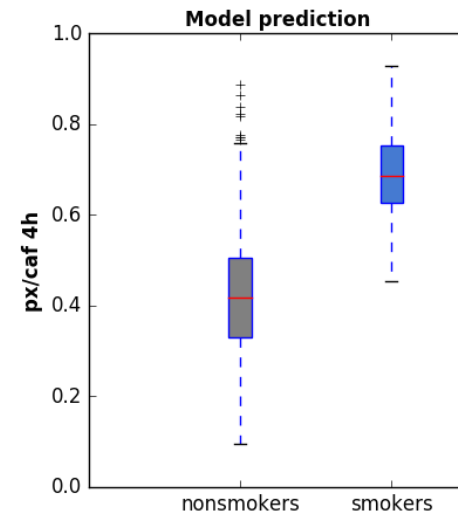
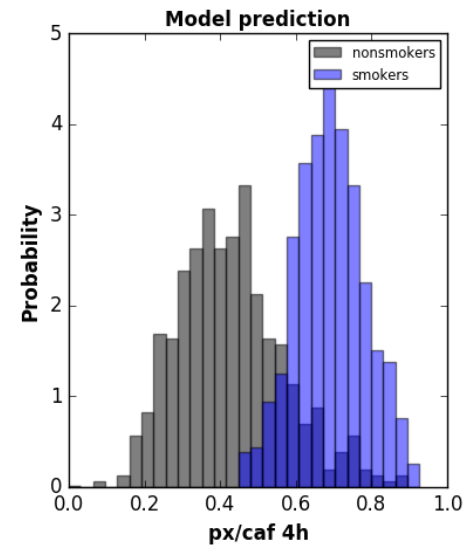
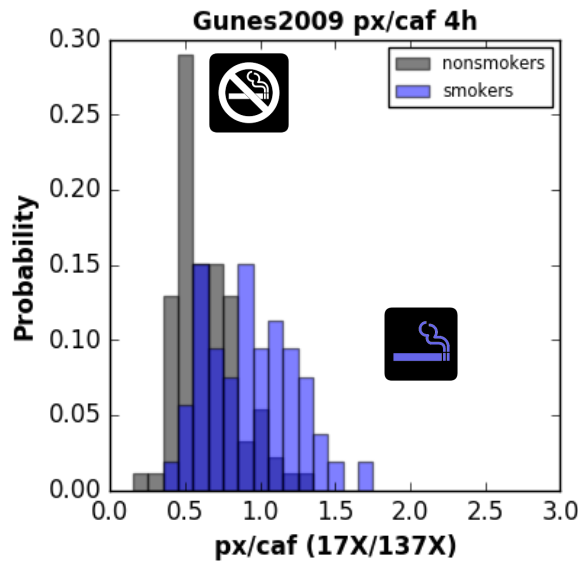
k_{el} : elimination rate



$t_{1/2}$: half-life

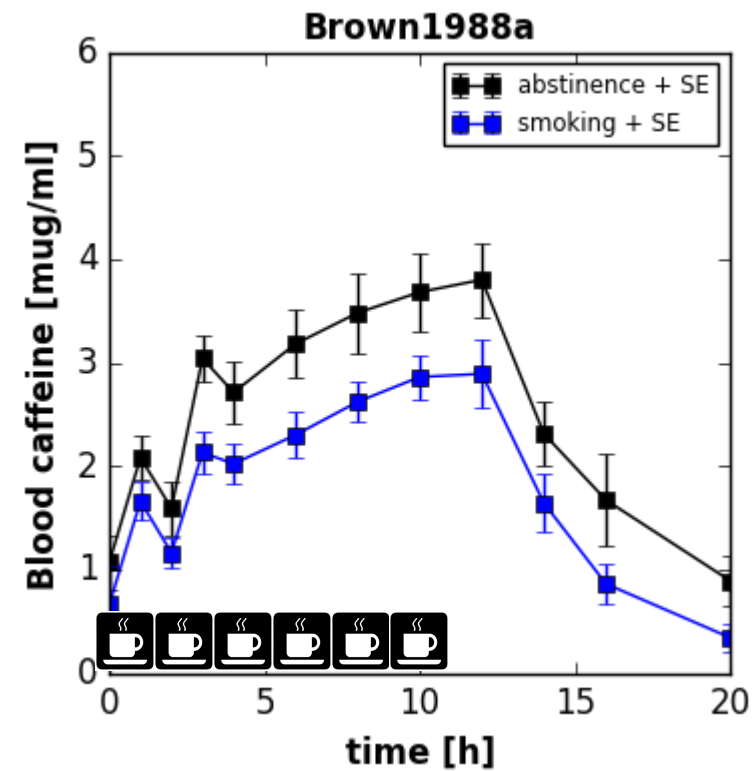
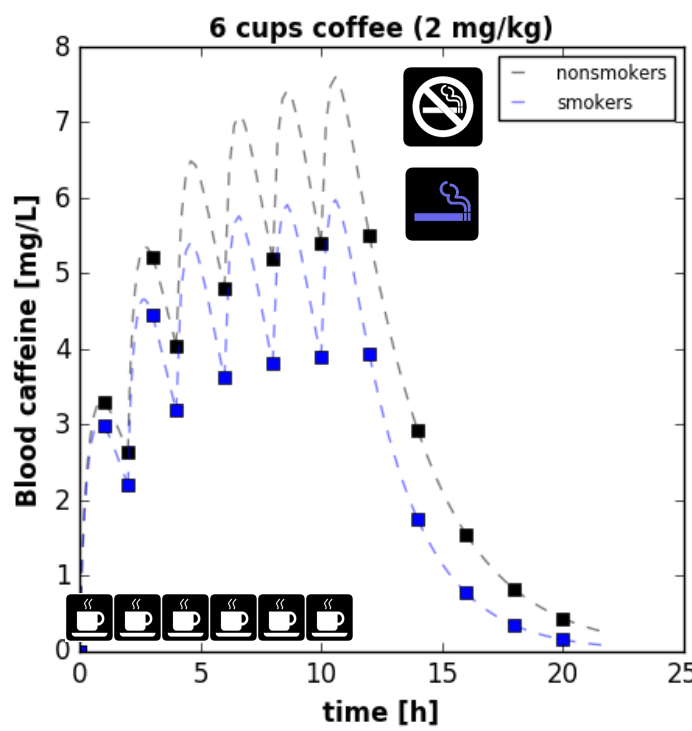


px/caf ratio (4h, 6h)



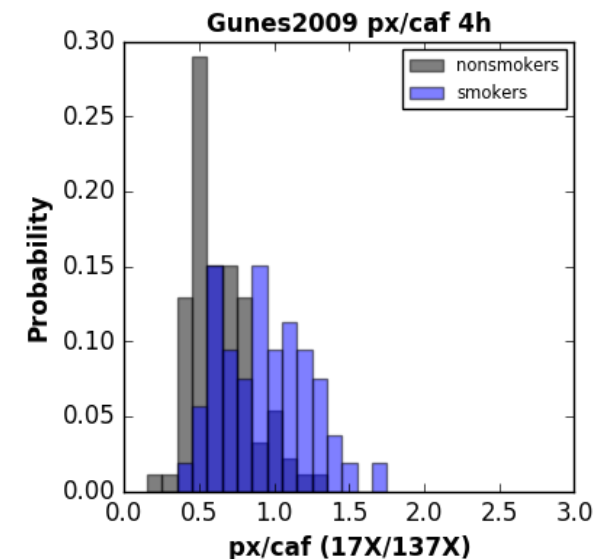
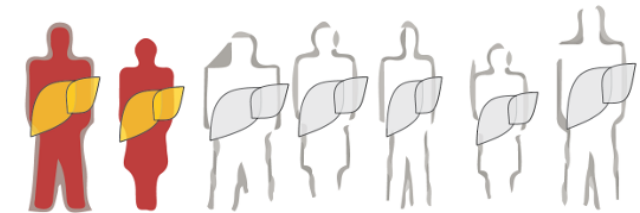
Prediction: coffee consume

- Multiple dosing
- Adaption to smoking status, i.e. high smokers, via dose response curve (CYP1A2 ~ smoking)



Work in progress

- **Model improvement**
high caffeine doses & paraxanthine doses
- **Metabolism of additional methyl-xanthines**
describe urinary profile and change of urinary metabolite ratios with smoking (CYP1A2 activity)
- **Simulating Virtual Populations**
organ volume & blood flow scaling, adapting to respective study populations
- **Coupling to logistic regression model**
Smoking one example of CYP1A2 induction effect
 - Contraceptives, coffee consumption, genetic variants
- **Further Validation with LiSyM drug cocktail**
Existing dataset of individual subject caffeine time courses. Testing predictive performance with personalized simulations (personalized PKPD model & regression adaption)



Caffeine Notebook

http://localhost:8888/notebooks/caffeine_pkpd/cafpkpd_model.ipynb

jupyter cafpkpd_model Last Checkpoint 2 minutes ago (autosaved) Python 2

PKPD model

PKPD model for clearance of caffeine by the human liver.

Caffeine and the primary metabolite paraxanthine are removed from the blood stream by hepatic or renal clearance. Caffeine can be given either as intra-venous injection or by oral dose.

TODO: create picture programmatically

```
In [1]: %matplotlib inline
from __future__ import print_function, division
import tellurium as te
from matplotlib import pyplot as plt
import pandas as pd
import numpy as np

# global settings for plots
plt.rcParams.update({
    'axes.labelsize': 'large',
    'axes.labelweight': 'bold',
    'axes.titlesize': 'large',
    'axes.titleweight': 'bold',
    'legend.fontsize': 'small',
    'xtick.labelszie': 'large',
    'ytick.labelszie': 'large',
})
```

LiSyM
Liver Systems Medicine

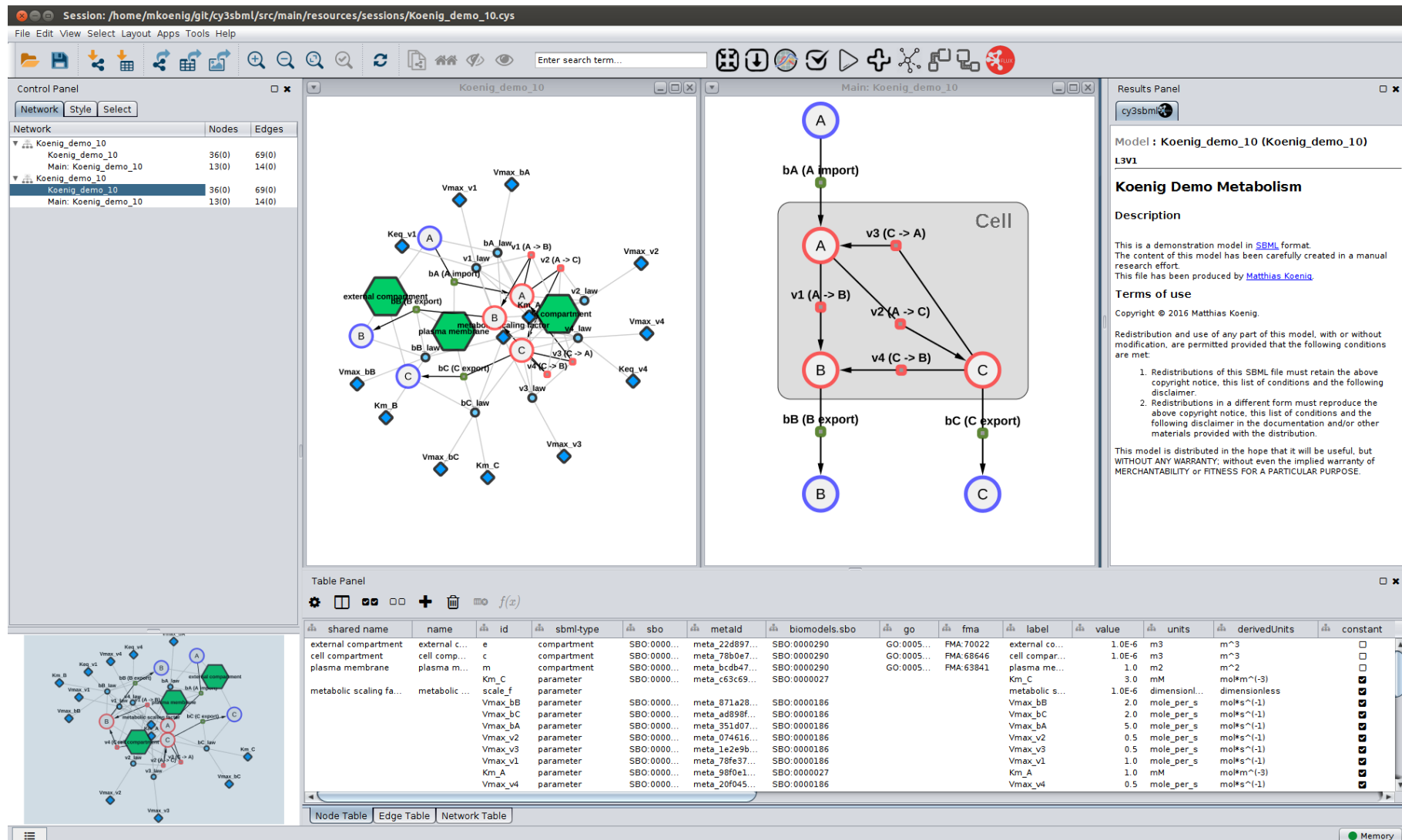
Model Standards



- SBML: Systems Biology Markup Language
 - Standard machine-readable format for model exchange
 - Reproducibility & Exchange of models
 - Re-usability
 - Annotations (Semantic information)
- Tool support
 - Simulators: COPASI, roadrunner
 - Model databases
 - Visualization
 - Analysis
 - ...

```
89   </listOfUnits>
90   </unitDefinition>
91 </listOfUnitDefinitions><listOfCompartments>
92   <compartment id="e" name="external compartment" spatialDimensions="3" size="1e-06" units="m<sup>3</sup>" constant="true"/>
93   <compartment id="c" name="cell compartment" spatialDimensions="3" size="1e-06" units="m<sup>3</sup>" constant="true"/>
94   <compartment id="m" name="plasma membrane" spatialDimensions="2" size="1" units="m<sup>2</sup>" constant="true"/>
95 </listOfCompartments><listOfSpecies>
96   <species id="c__A" name="A" compartment="c" initialConcentration="0" substanceUnits="mole_per_l" constant="true"/>
97   <species id="c__B" name="B" compartment="c" initialConcentration="0" substanceUnits="mole_per_l" constant="true"/>
98   <species id="c__C" name="C" compartment="c" initialConcentration="0" substanceUnits="mole_per_l" constant="true"/>
99   <species id="e__A" name="A" compartment="e" initialConcentration="10" substanceUnits="mole_per_l" constant="true"/>
100  <species id="e__B" name="B" compartment="e" initialConcentration="0" substanceUnits="mole_per_l" constant="true"/>
101  <species id="e__C" name="C" compartment="e" initialConcentration="0" substanceUnits="mole_per_l" constant="true"/>
102 </listOfSpecies><listOfParameters>
103  <parameter id="scale_f" name="metabolic scaling factor" value="1e-06" units="dimensionless" constant="true"/>
104  <parameter id="Vmax_bA" value="5" units="mole_per_s" constant="true"/>
105  <parameter id="Km_A" value="1" units="mM" constant="true"/>
106  <parameter id="Vmax_bb" value="2" units="mole_per_s" constant="true"/>
107  <parameter id="Km_B" value="0.5" units="mM" constant="true"/>
108  <parameter id="Vmax_bc" value="2" units="mole_per_s" constant="true"/>
109  <parameter id="Km_C" value="3" units="mM" constant="true"/>
110  <parameter id="Vmax_v1" value="1" units="mole_per_s" constant="true"/>
111  <parameter id="Keq_v1" value="10" units="dimensionless" constant="true"/>
112  <parameter id="Vmax_v2" value="0.5" units="mole_per_s" constant="true"/>
113  <parameter id="Vmax_v3" value="0.5" units="mole_per_s" constant="true"/>
114  <parameter id="Vmax_v4" value="0.5" units="mole_per_s" constant="true"/>
115  <parameter id="Keq_v4" value="2" units="dimensionless" constant="true"/>
116 </listOfParameters><listOfReactions>
117  <reaction id="bA" name="bA (A import)" reversible="false" fast="false" compartment="m">
118    <listOfReactants>
119      <speciesReference species="e__A" stoichiometry="1" constant="true"/>
120    </listOfReactants>
121    <listOfProducts>
122      <speciesReference species="c__A" stoichiometry="1" constant="true"/>
123    </listOfProducts>
124    <kineticLaw>
125      <math xmlns="http://www.w3.org/1998/Math/MathML" xmlns:	sbml="http://www.sbml.org/sbml/level3/version1/kinetic/definition">
126        <apply>
127          <divide/>
```

Visualization & Data Integration



König

cy3sabiork: A Cytoscape app for visualizing kinetic data from SABIO-RK

2016 [version 1; referees: 2 approved with reservations]

<http://f1000research.com/articles/5-1736/v1>

<https://github.com/matthiaskoenig/cy3sabiork>

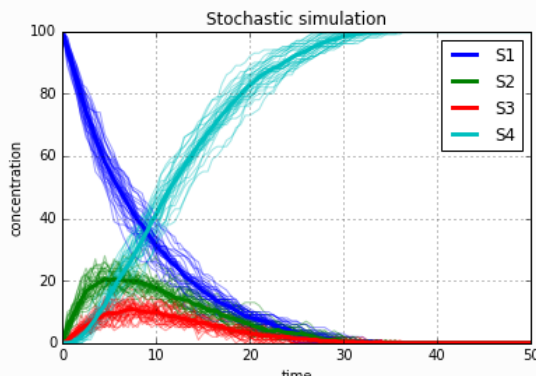
König, Rodriguez, and Dräger
cy3sbml: A Cytoscape app for SBML
2016, manuscript in preparation

<https://github.com/matthiaskoenig/cy3sbml>



Modeling Tools

```
r = te.loada(''  
J1: S1 -> S2; k1*S1;  
J2: S2 -> S3; k2*S2 - k3*S3  
# J2_1: S2 -> S3; k2*S2  
# J2_2: S3 -> S2; k3*S3;  
J3: S3 -> S4; k4*S3;  
  
k1 = 0.1; k2 = 0.5; k3 = 0.5; k4 = 0.5;  
S1 = 100;  
'')  
  
# set integrator, seed and selections for output  
r.setIntegrator('gillespie')  
r.setSeed(1234)  
r.selections = ['time'] + r.getBoundarySpeciesIds() + r.getFloatingSpeciesIds()  
  
# run repeated simulation  
Ncol = len(r.selections)  
Nsim = 30  
points = 101  
s_sum = np.zeros(shape=[points, Ncol])  
for k in range(Nsim):  
    r.resetToOrigin()  
    s = r.simulate(0, 50, points)  
    s_sum += s  
# no legend, do not show  
r.plot(s, show=False, loc=None, alpha=0.4, linewidth=1.0)  
  
# add mean curve, legend, show everything and set labels, titels, ...  
s_mean = s_sum/Nsim  
r.plot(s_mean, loc='upper right', show=True, linewidth=3.0,  
       title="Stochastic simulation", xlabel="time", ylabel="concentration", grid=True);
```



- High performance simulators based on SBML
- Python based modeling environment

Choi K., Medley JK., Cannistra C., **König M.**, Smith L., Stocking K., and Sauro HM.
Tellurium: A Python Based Integrated Environment for Biological Modeling and Simulation

[2016, accepted]

Somogyi, Bouteiller, Glazier, **König**, Medley, Swat, Sauro.
libRoadRunner: a high performance SBML simulation and analysis library.

Bioinformatics. 2015

<https://github.com/sys-bio/roadrunner>

LiMAX (Metacethin)

M.König, T. Wünsch & Prof. Stockmann

LiMAX

- **LiMAX PKPD model:**
methacetin, paracetamol, CO₂
- **Model calibration**
 - Existing timecourse data of methacetin, paracetamol, DOB
 - Existing studies to paracetamol & CO₂ distribution
- **Analysis: Effect of smoking on LiMAX results & test correction for smoking**
 - CYP1A2 substrate (analog changes like caffeine)
 - Model validation with retrospective analysis of LiMAX data

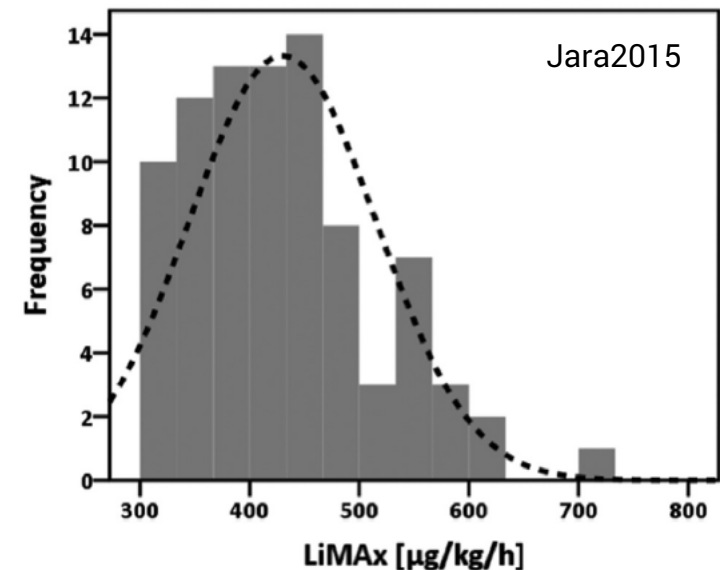
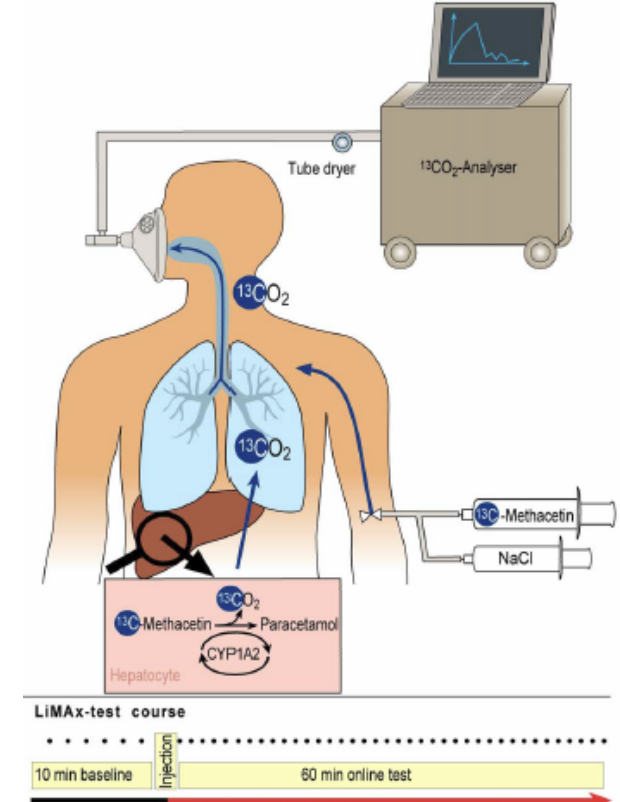
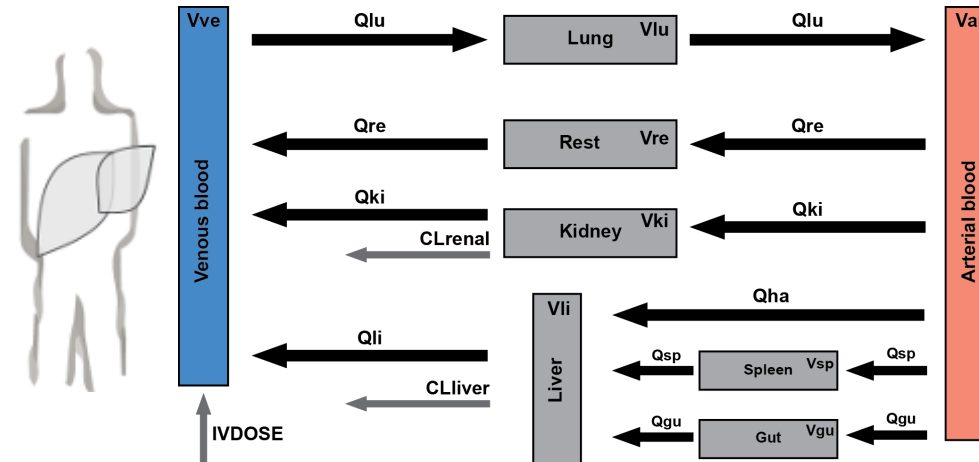


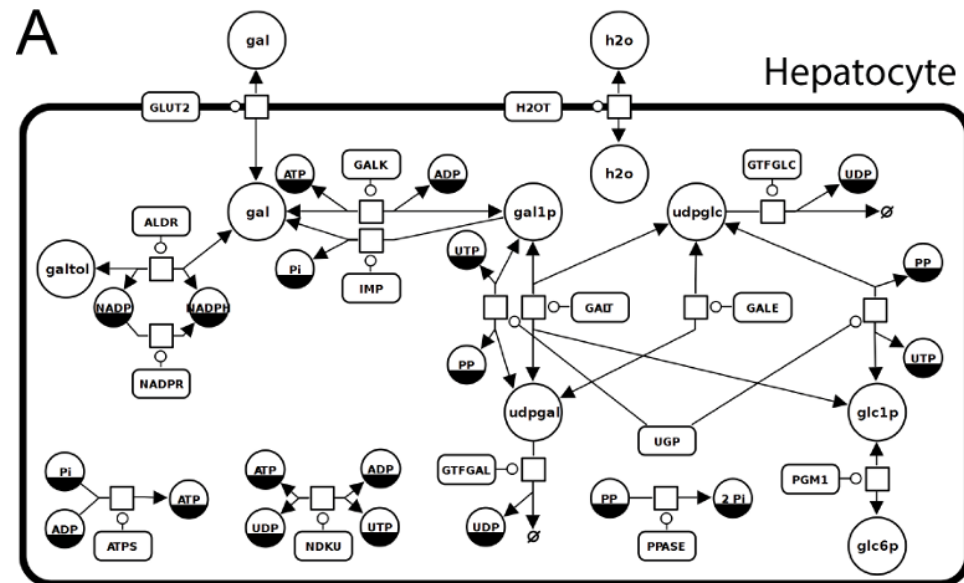
Fig. 1 – Distribution of LiMAX values in 86 healthy volunteers.

Galactose (GEC)

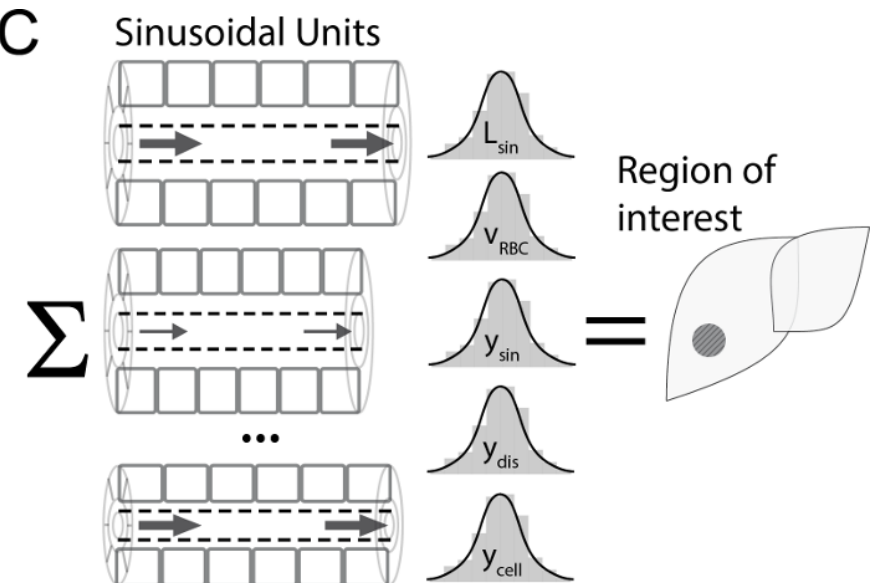
König, Marchesini, Bianchi, Holzhütter

Galactose Elimination Capacity

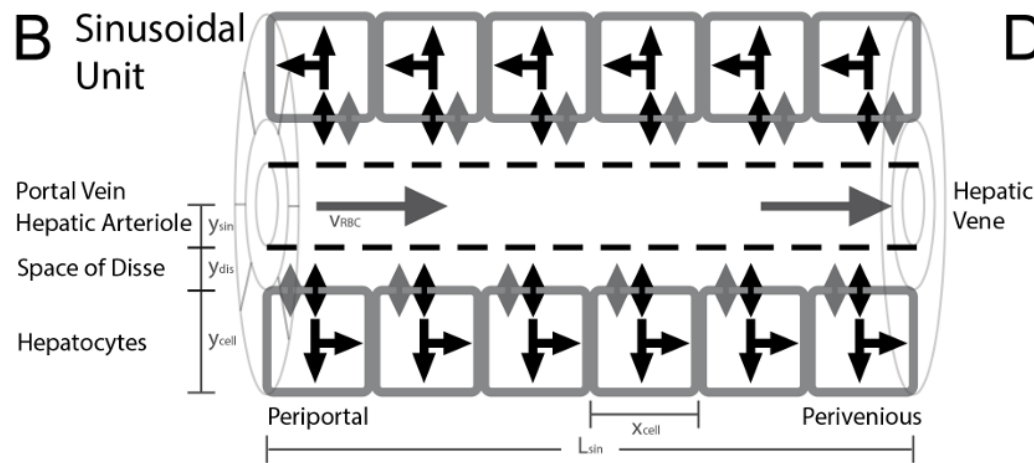
A



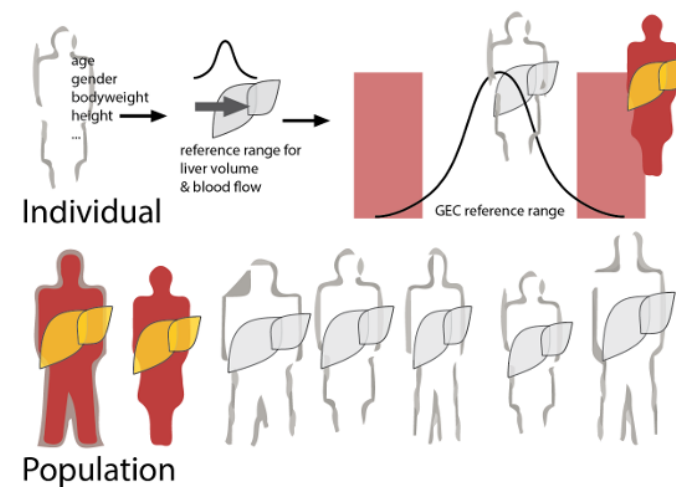
C



B Sinusoidal Unit



D

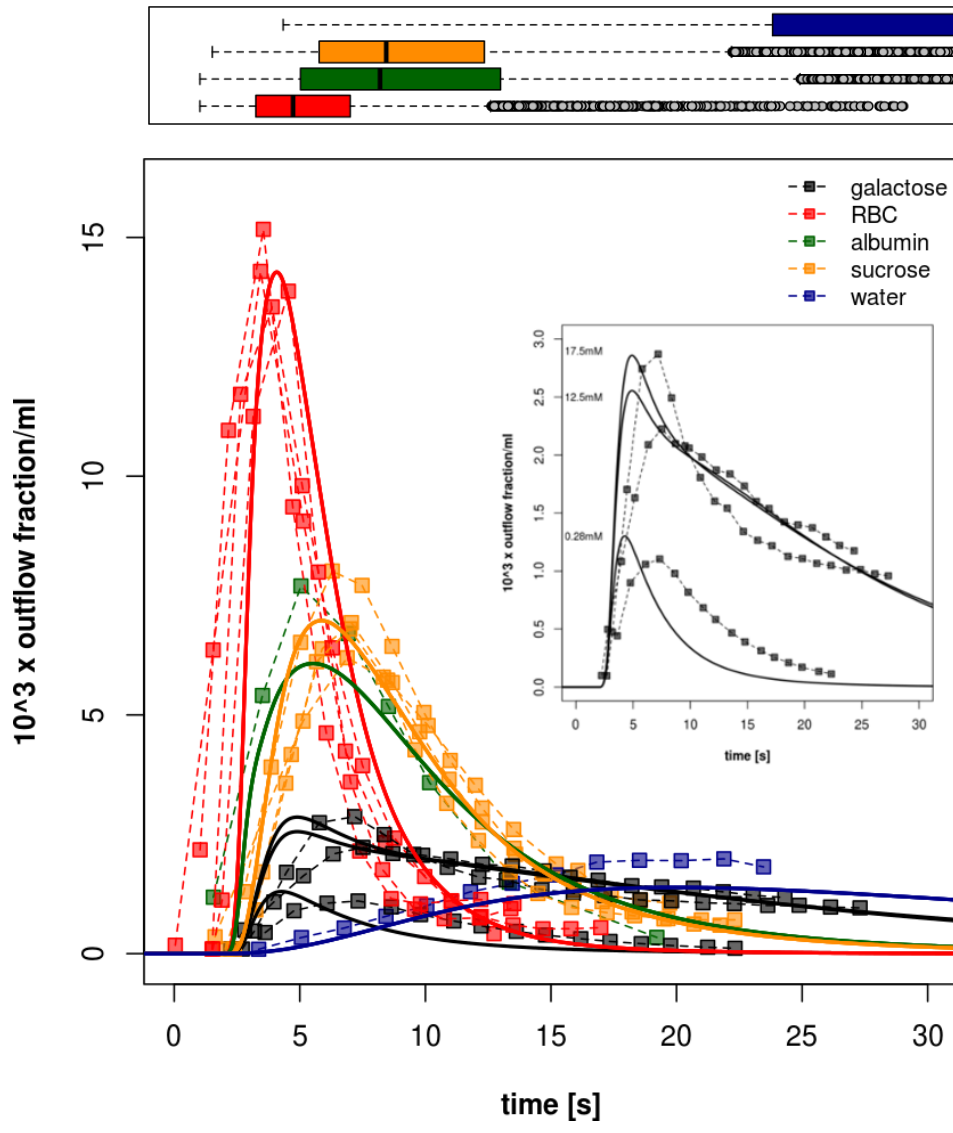


König M., Marchesini G., Bianchi G. and Holzhütter HG.

A Multiscale Computational Model Predicts Human Liver Function From Single-Cell Metabolism
2017, [manuscript in preparation]

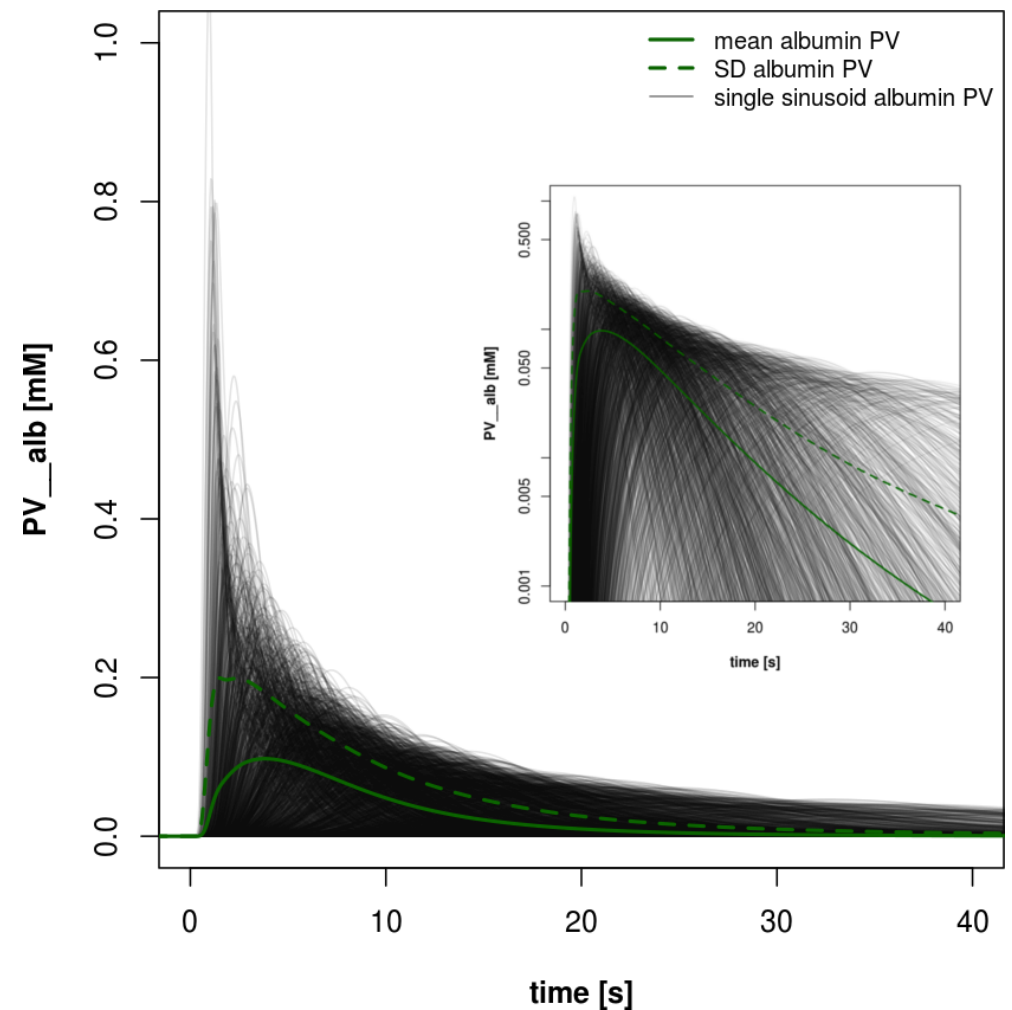
Multiple Indicator Dilution

Input-Output profile after test substances



Heterogeneity

- Liver function depends strongly on local liver perfusion, ultrastructure & test substance

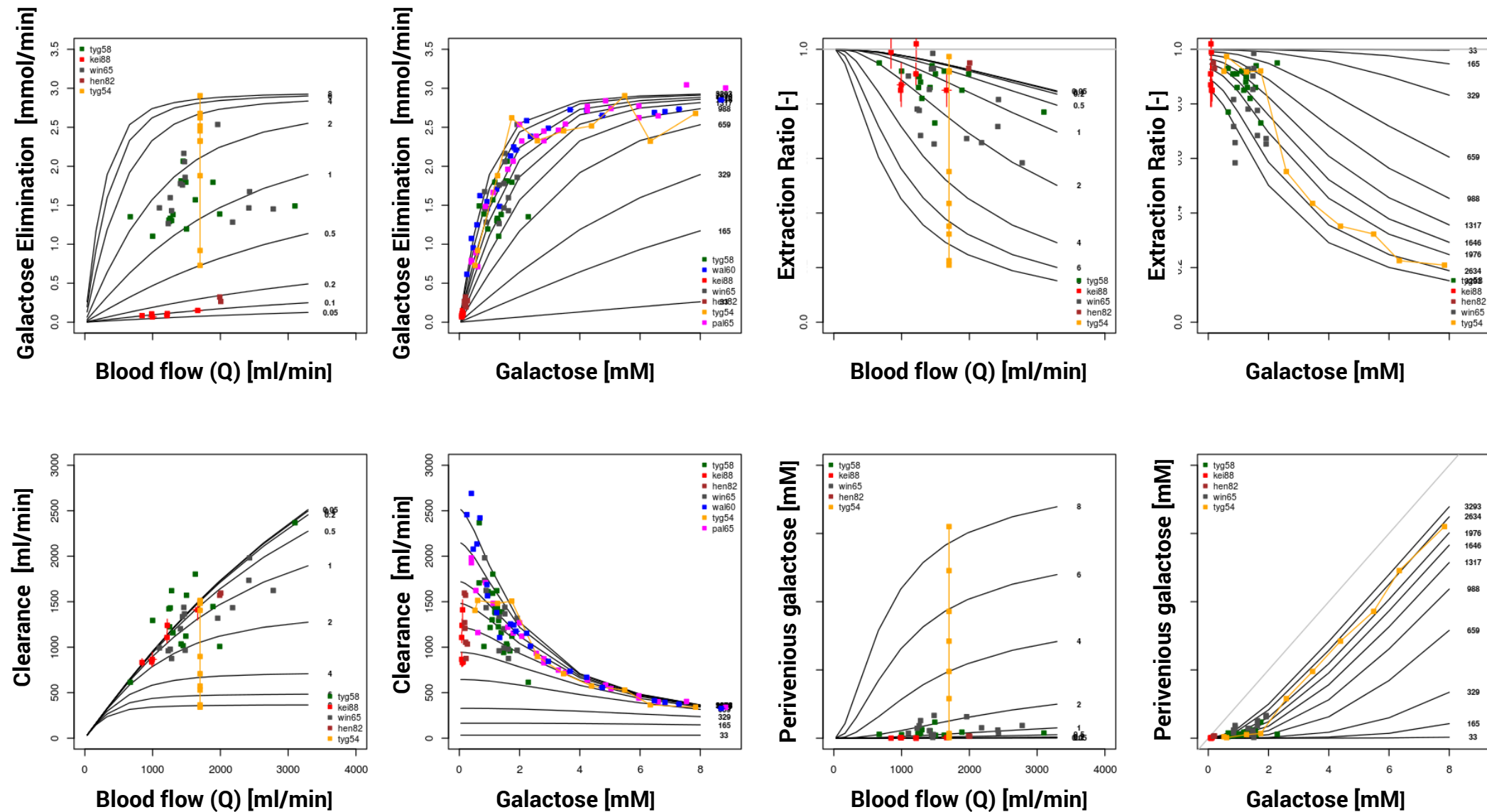


Liver Galactose elimination, extraction ratio & clearance

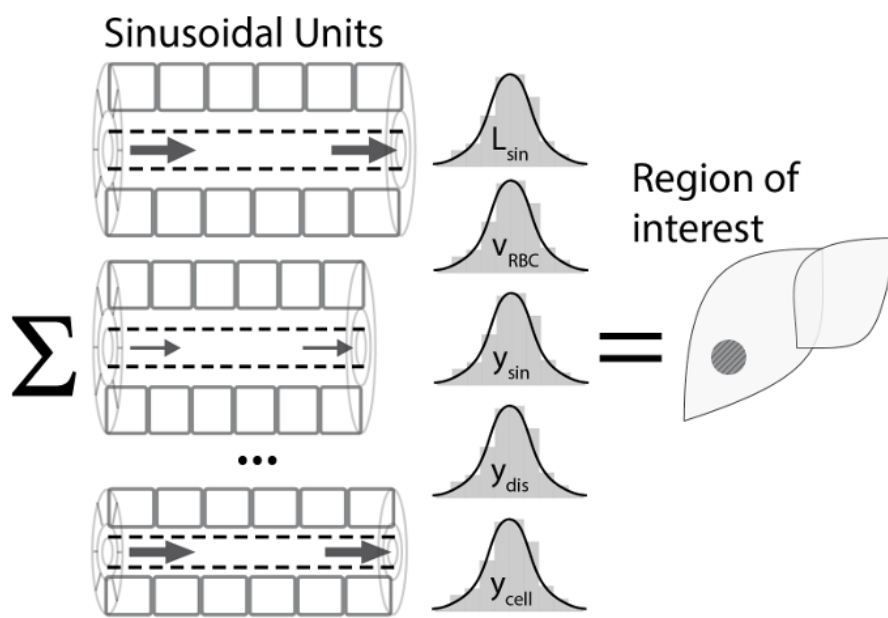
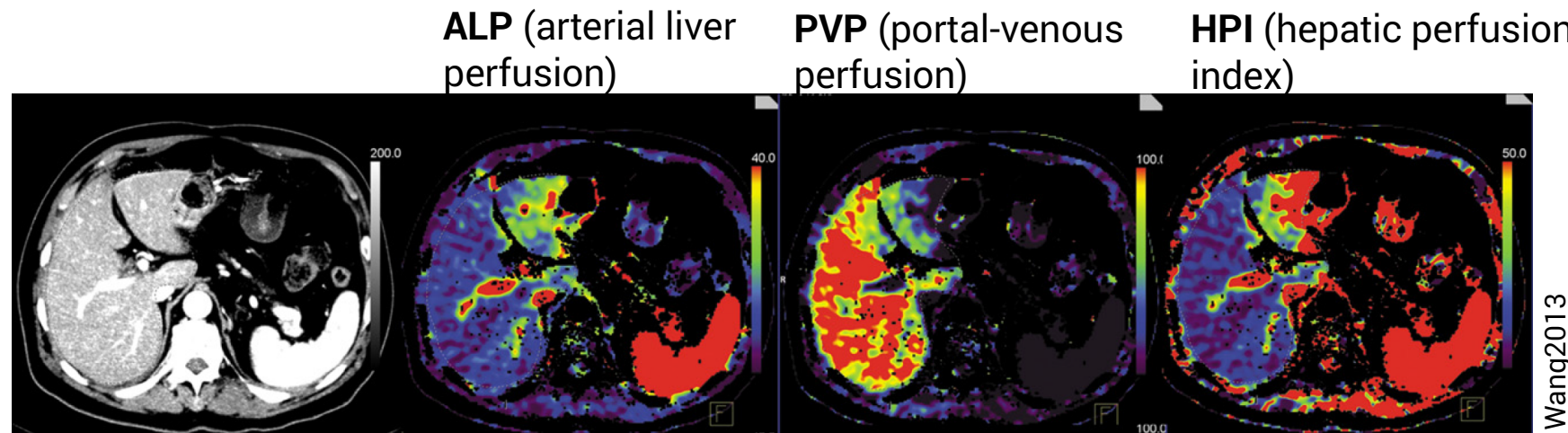
$$GE[k] = Q_{sin}[k](c_{pp}^{gal}[k] - c_{pv}^{gal}[k])$$

$$ER[k] = \frac{c_{pp}^{gal}[k] - c_{pv}^{gal}[k]}{c_{pp}^{gal}[k]}$$

$$CL[k] = Q_{sin}[k] \frac{c_{pp}^{gal}[k] - c_{pv}^{gal}[k]}{c_{DD}^{gal}[k]} = Q_{sin}[k] ER[k]$$

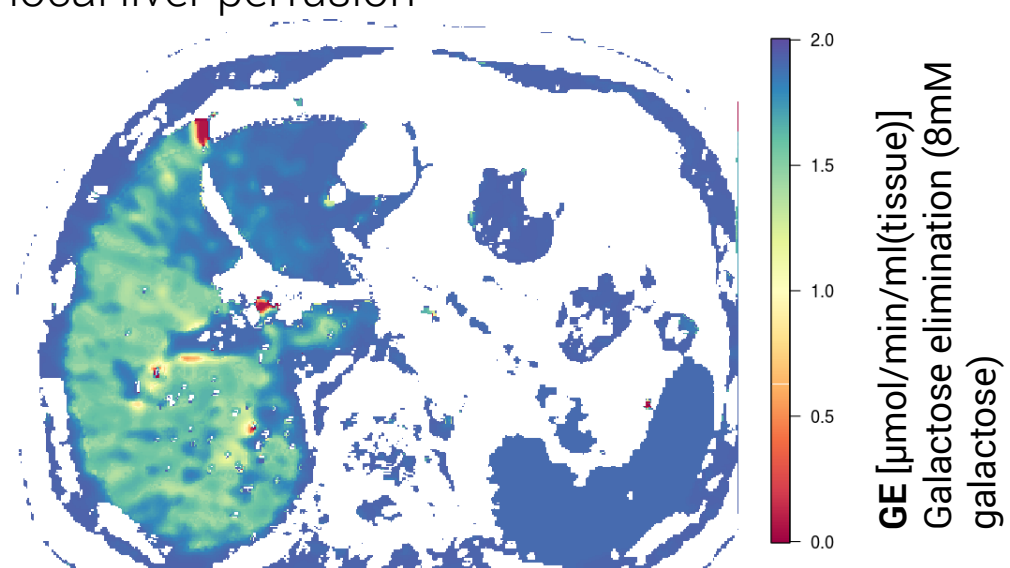


Spatial galactose elimination



Perfusion CTs

- Galactose elimination depending on local liver perfusion



Personalized prediction

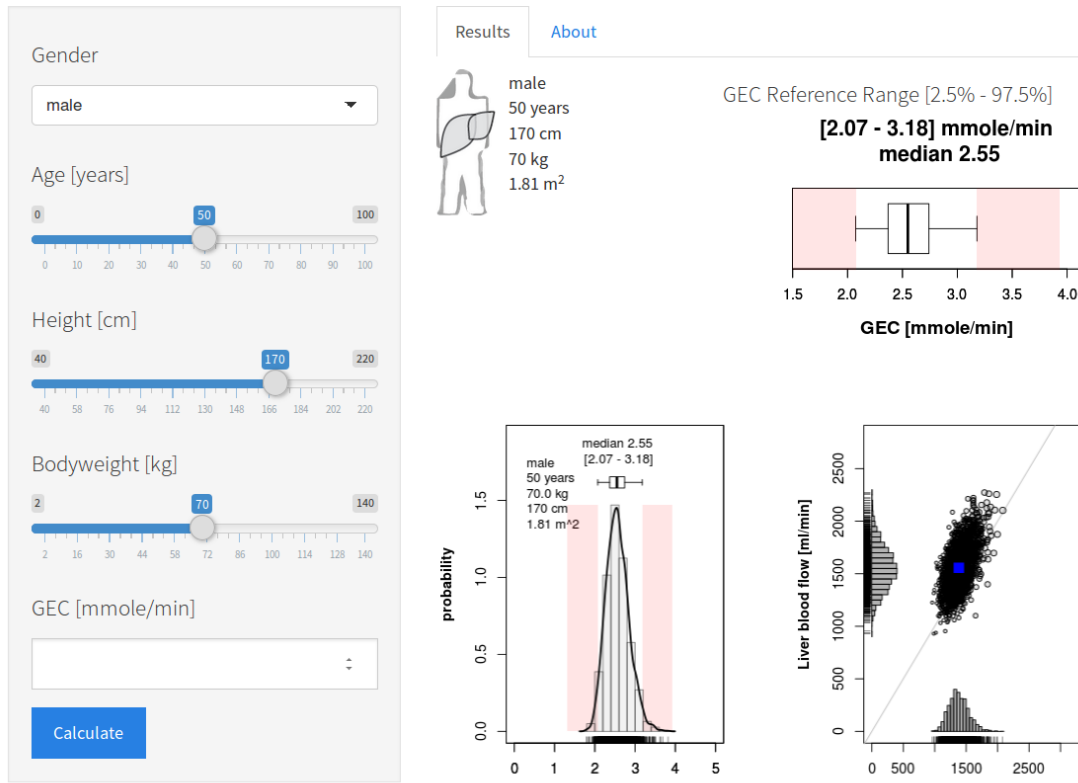


Individual evaluation of liver function test

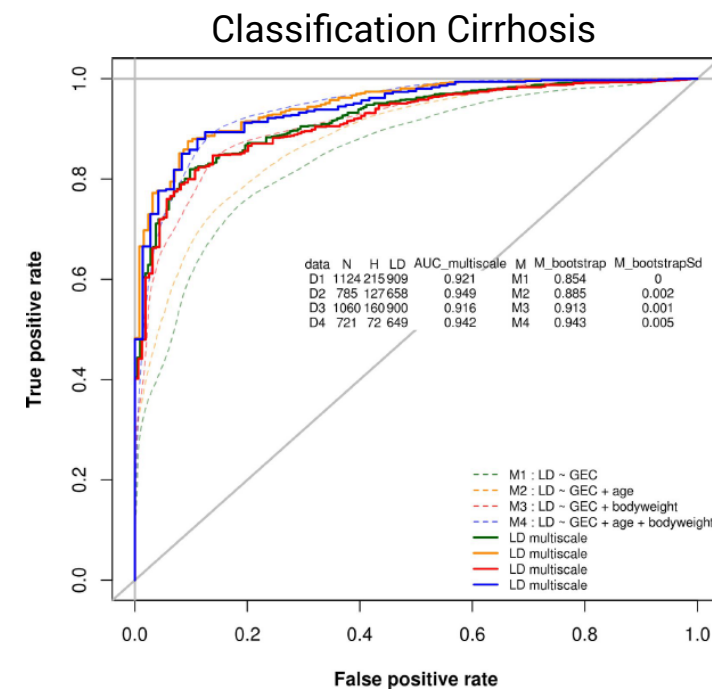
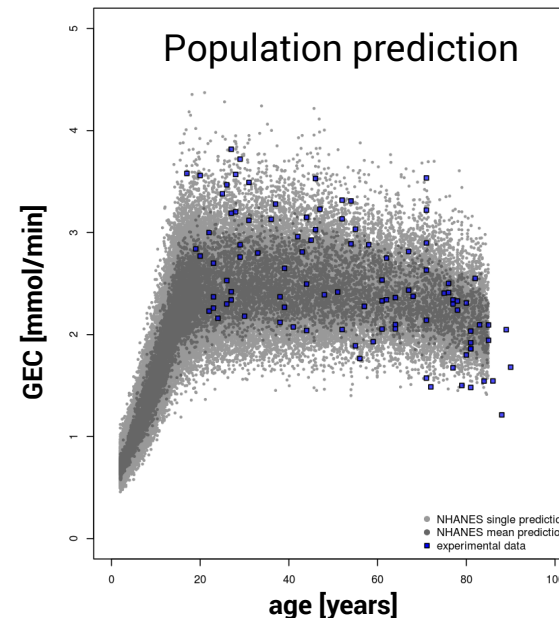
- Simulation of *in silico* population representative of the individual subject



Galactose Elimination Capacity (GEC)



GEC App



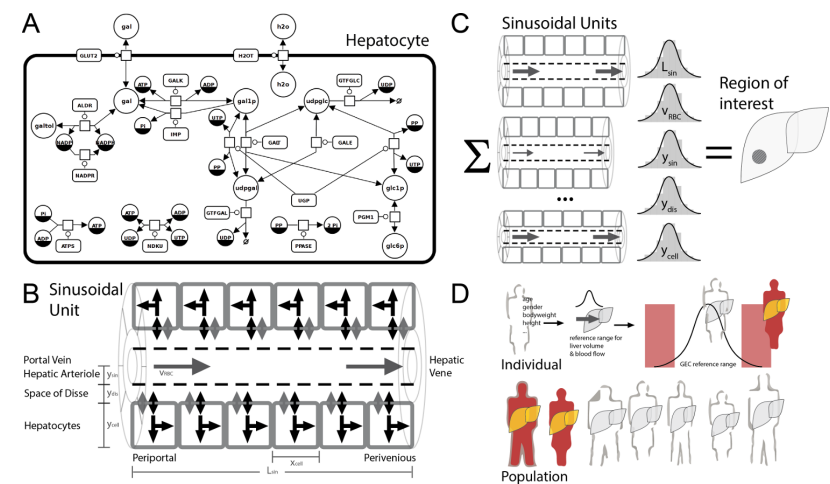
Outlook

Integration with PKPD models

- time courses of whole-body distribution and urinary extraction
- *In silico* trials & virtual populations
- Large dataset of individual subject galactose time courses for analysis (Marchesini)

Integration CT data

- Simulate spatial heterogeneity in liver function
- Integration with perfusion CT, functional CT (Keiding?)



Acknowledgement

- Prof. Holzhütter
- Prof. Marchesini & Prof. Gianchi
- Tilo Wünsch & Prof. Stockmann
- Researchers which make their data accessible
(you are the real heros)



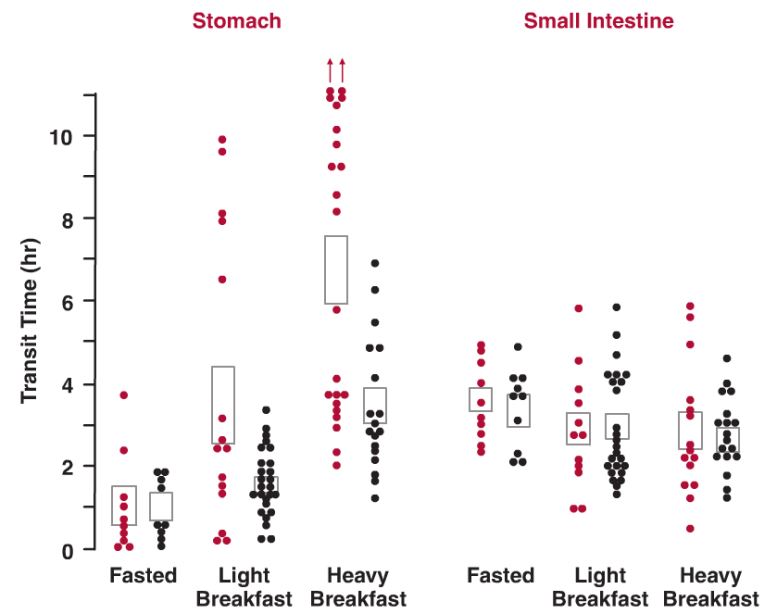


FIGURE 7-10. Food, particularly a heavy meal, increases the gastric transit time of small pellets (black circles) and, even more markedly, of large single pellets (colored circles). In contrast, neither the food nor the physical size of the solid affects the small intestine transit time. The data (individual points, black or colored circles, and their mean \pm S.E., indicated by the rectangles) were obtained in healthy young adults using drug-free nondisintegrating materials. The points with an arrow indicate that the solid was still in the stomach at the time of the last observation, 16 hr. (From: Davis SS, Hardy JG, Fara JW. Transit of pharmaceutical dosage forms through the small intestine. Gut, 1986;27:886–892.)

Smoking cessation

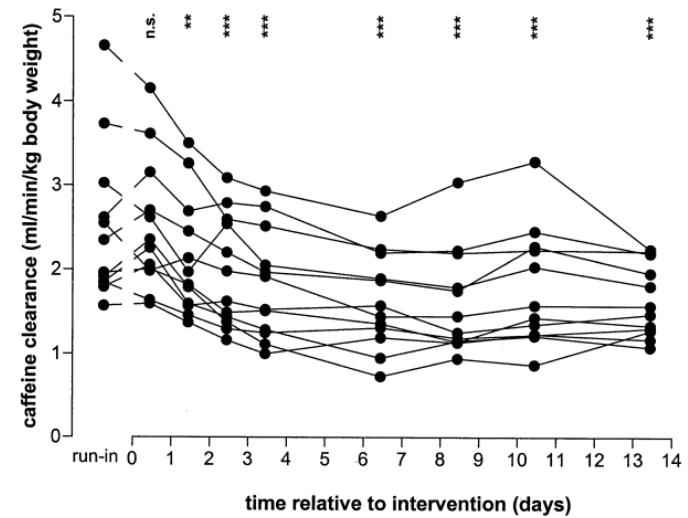
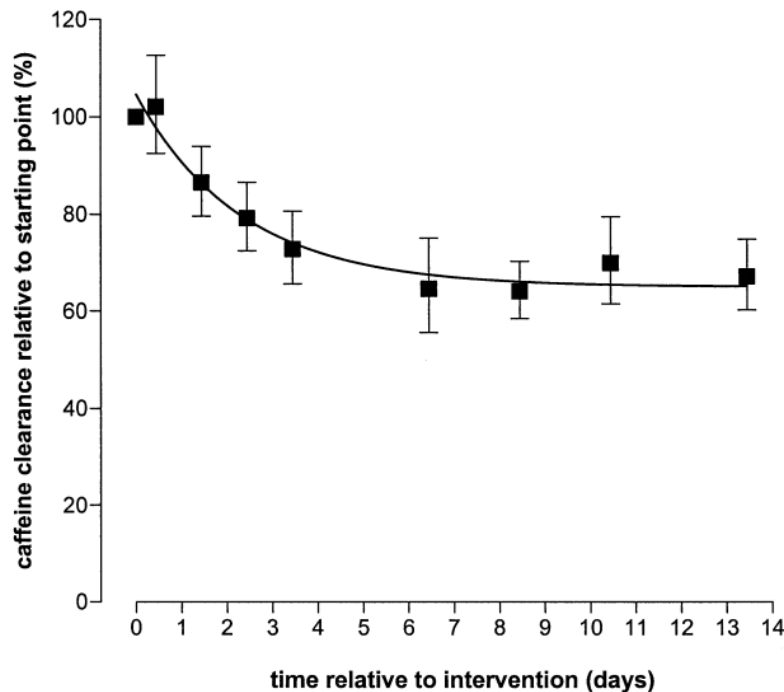
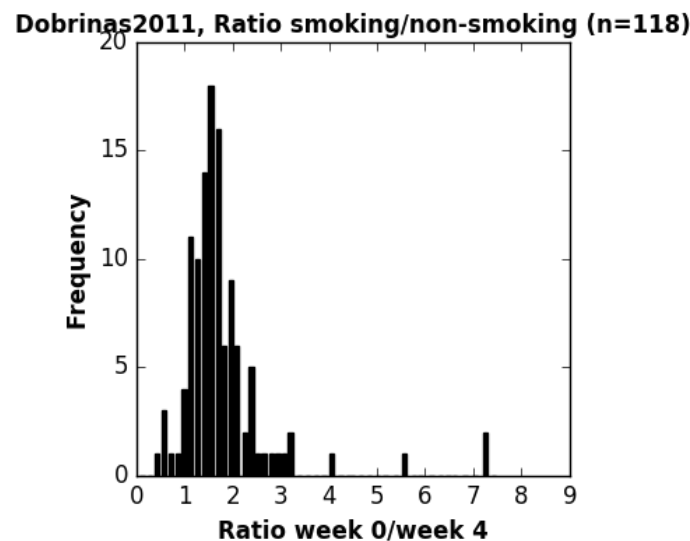


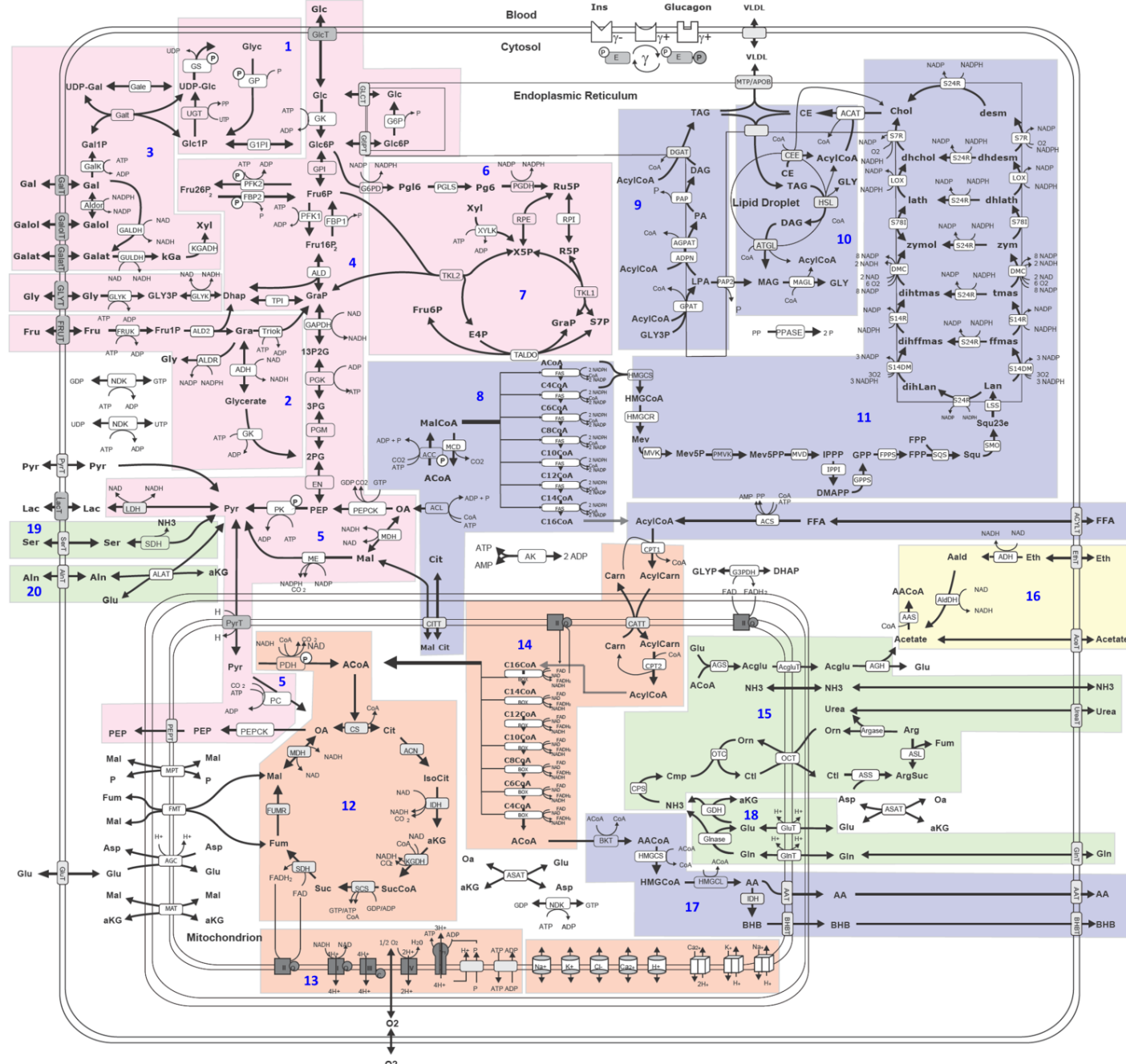
Fig 1. Individual time courses of caffeine clearance estimated from paraxanthine/caffeine plasma ratios after the intervention of smoking cessation. The “run-in” value is the individual geometric mean of values on days -6 , -4 , and -1 . ns, Not significant ($P \geq .05$); 2 asterisks, $P < .005$; 3 asterisks, $P < .0005$; these are for descriptive comparisons relative to individual starting points by use of 2-sided t tests for paired samples.



WP3 Central Carbon Model

- Kinetic model of central liver metabolism

Berndt N., Bulik S., Wallach I.,
König M., Stockmann M.,
Meierhofer D. and Holzhütter HG.
Computational Assessment of Liver Metabolism
[2016, manuscript in preparation]



WP3 Metabolic Modeling Liver

- Kinetic models
(glucose & central metabolism, detoxification)
- Flux Balance Analysis
Genome-scale liver
- Hybrid approaches

König M. and Holzhütter HG.
Homeostasis of blood glucose - Computer simulations of central liver functions.
systembiologie.de 2014; 8:p.53-57

König M. and Holzhütter HG.
Kinetic Modeling of Human Hepatic Glucose Metabolism in T2DM Predicts Higher Risk of Hypoglycemic Events in Rigorous Insulin Therapy

J Biol Chem. 2012

König M., Bulik S. and Holzhütter HG.
Quantifying the Contribution of the Liver to the Homeostasis of Plasma Glucose: A Detailed Kinetic Model of Hepatic Glucose Metabolism Integrated with the Hormonal Control by Insulin, Glucagon and Epinephrine

PLoS Comput Biol. 2012

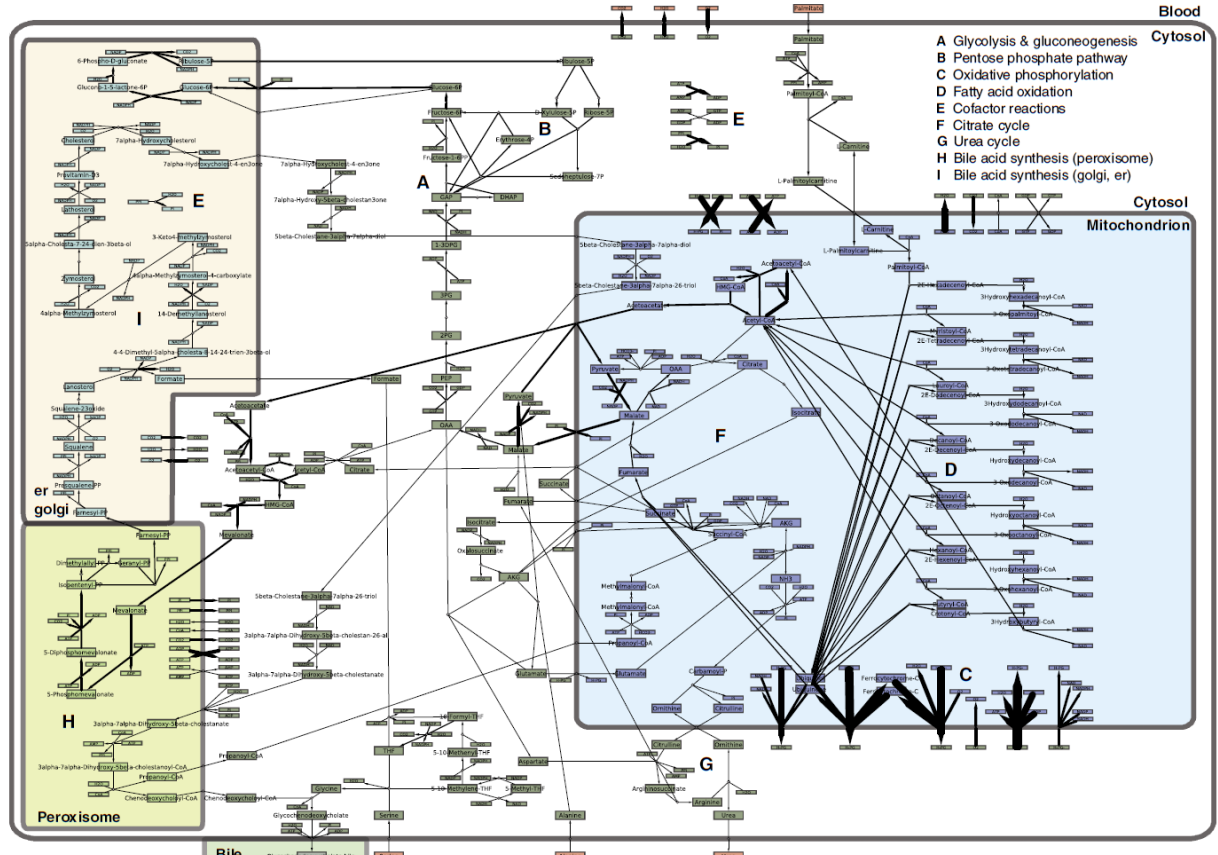


Figure 1 Functional flux mode for the synthesis of glycocholate. Flux distribution obtained for canalicular glycocholate as target flux using the minimal exchange set. Metabolites are labeled and color coded according to their sub-cellular localization (s, sinusoidal; c, cytosol; r, endoplasmic reticulum; m, mitochondrion; b, bile). All internal metabolites are balanced, including cofactors, which may appear in several instances in the graph. Reaction arrows correspond to flux direction and magnitude predicted by TR-FBA and reaction identifiers are indicated. The flux graph was created with the program CytoScape (Shannon et al., 2003; Kilcoyne et al., 2009) and our own CytoScape plug-in FluxViz (König and Holzhütter, 2010).

Gille C, Bölling C, Hoppe A, Bulik S, Hoffmann S, Hübner K, Karlstädt A, Ganeshan R,

König M, Rother K, Weidlich M, Behre J, Holzhütter HG.

HepatoNet1: a comprehensive metabolic reconstruction of the human hepatocyte for the analysis of liver physiology.

Mol Syst Biol., 6:411., 2010

Junior Group LiSyM: Multi-scale Modeling for Personalized Liver Function Tests

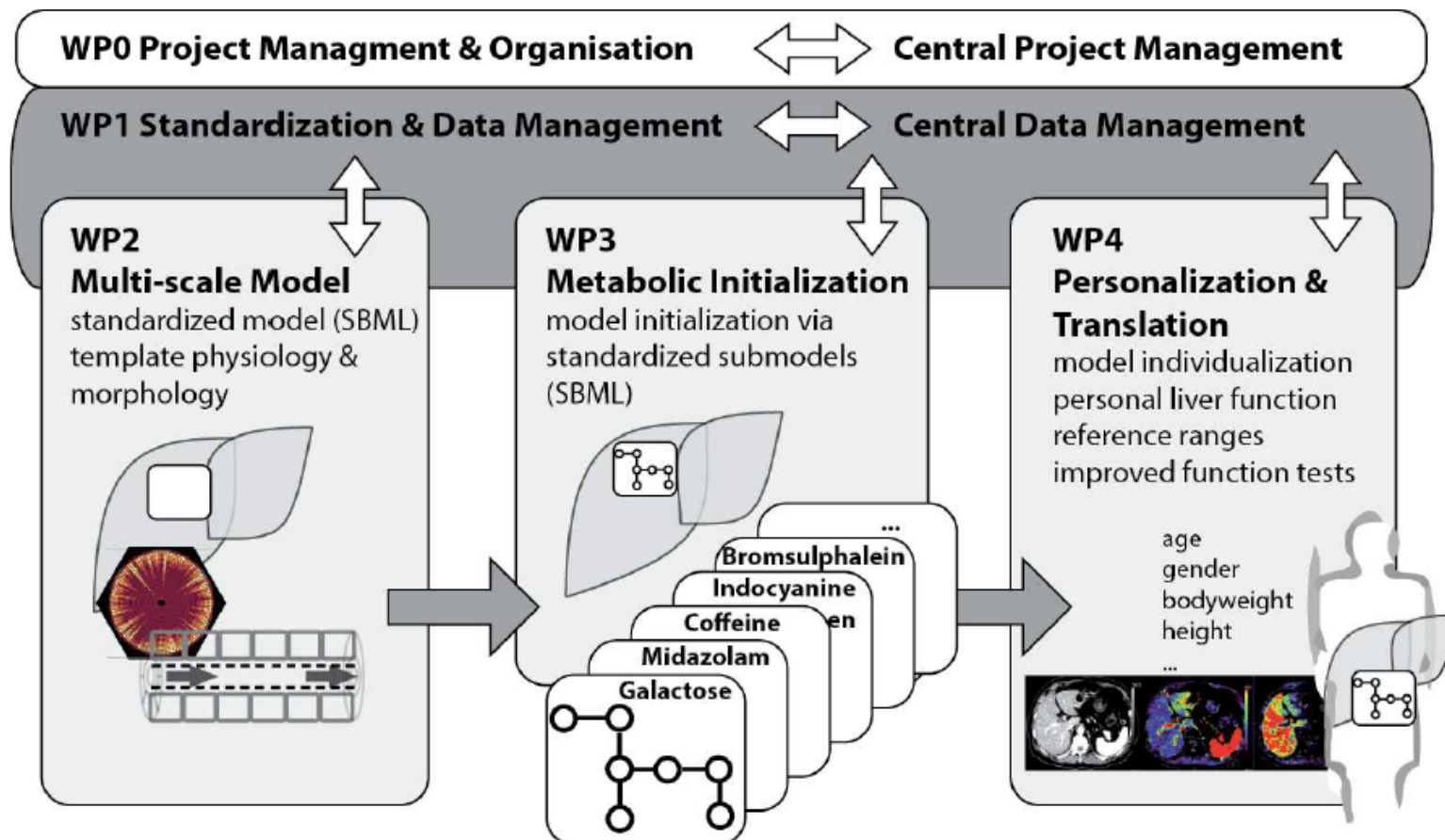


Figure 1 - Overview of the five work packages and their interconnection with description provided in the main text. The standardization of all data and workflows is crucial for the individual work packages. All data will be managed via central standardized data management.

WP1 Standardization

- Reproducible Computational Research
- Application of standard formats
- Integration of clinical/patient data with computational models

König M.*, Oellrich A.*¹, Waltemath D.*¹,
Dobson R., Hubbard T., and Wolkenhauer O.

* equal contribution

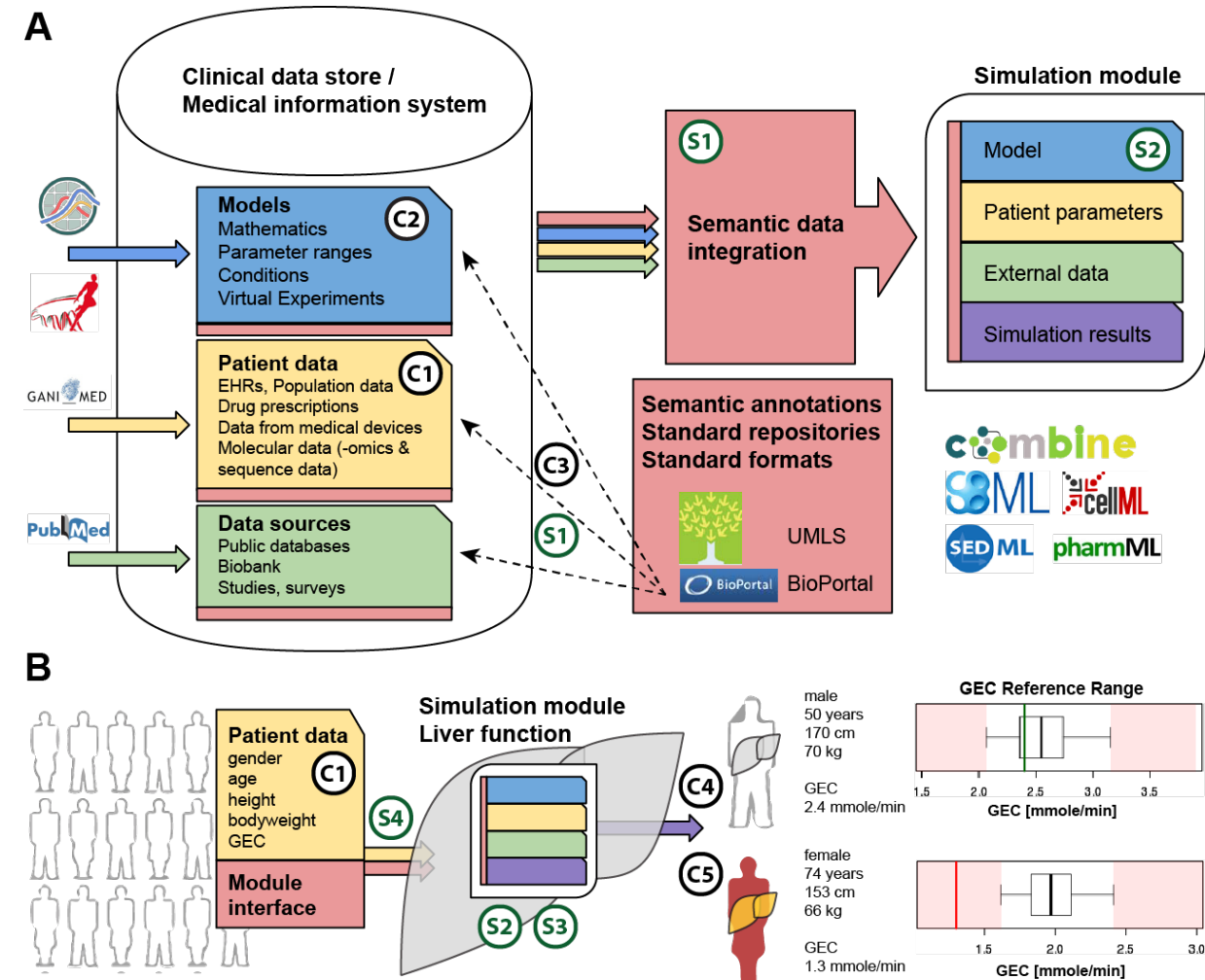
Challenges and opportunities for system biology standards and tools in medical research

[2016, accepted]

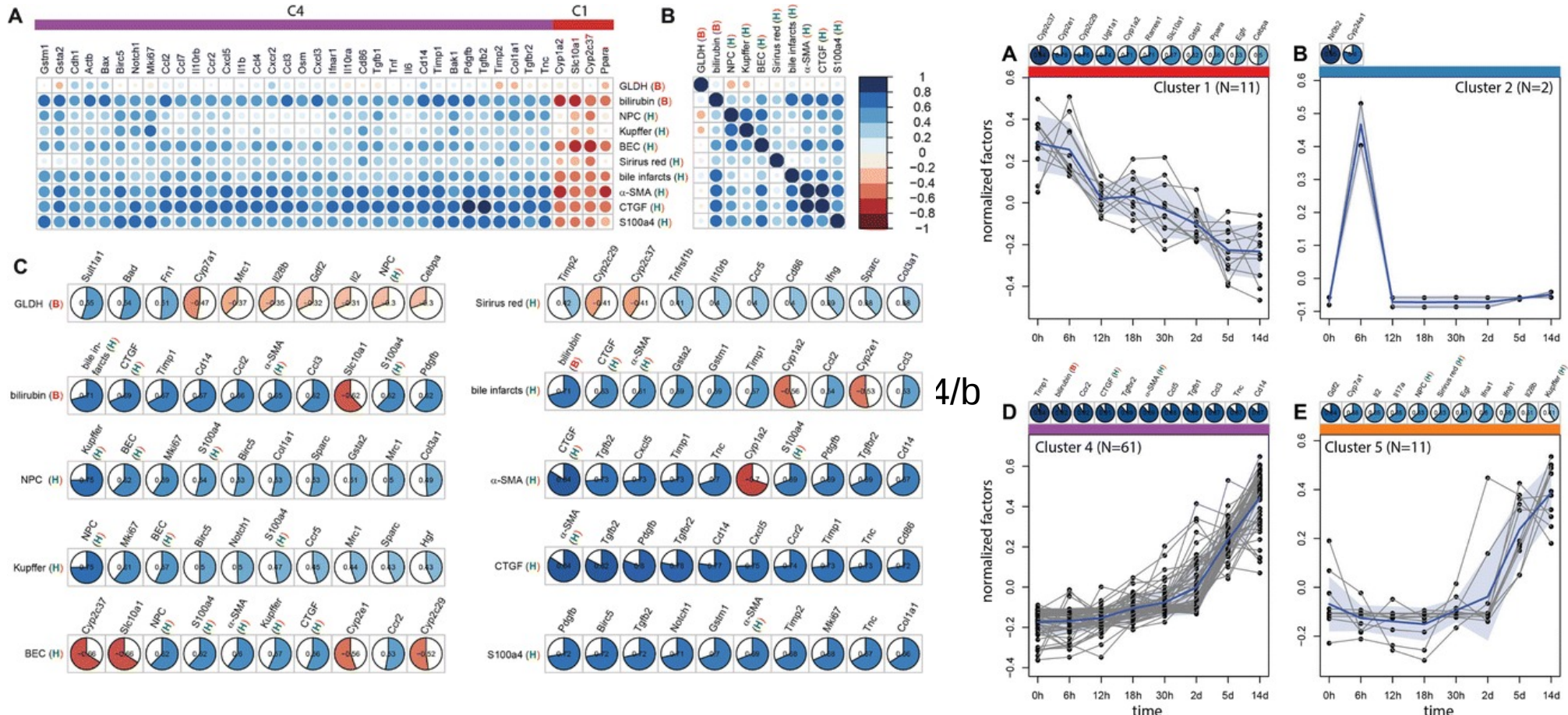
Wholecell Consortium (König M.)

Toward community standards and software for whole-cell modeling

IEEE Trans Biomed Eng. 2016 Jun 10.



Bioinformatics Analyses



Abshagen*, König*, Hoppe A., Thomas M., Müller I., Ebert M., Weng H., Holzhütter HG., Zanger UM., Bode J., Vollmar B. and Dooley S.

* equal contribution

Pathobiochemical signatures of cholestatic liver disease in bile duct ligated mice

2015, BMC Systems Biology

<https://github.com/matthiaskoenig/bdl-analysis>

- Circadian omics data & Integration metabolic models

Patrick Pett, Hanspeter Herzel, Matthias König
Circadian rhythms in the mouse liver

Ultrastructural changes in aging

Pseudocapillarization

- Endothelial cells are thickened and defenestrated with old age

		Human
fenestration radius $\frac{r_{fen}^{old}}{r_{fen}^{young}}$	1.0 old (60 years)/young (20 years)	diameter 58±1nm (young, baboon), 70±2nm (old, baboon), old/young 1.21
porosity $\frac{f_{fen}^{old}}{f_{fen}^{young}}$	0.25 old (60 years)/young (20 years)	porosity determined by scanning electron microscopy 4.2±0.5% (young, baboon), 2.4±0.4% (old, baboon), old/young 0.61
frequency $\frac{N_{fen}^{old}}{N_{fen}^{young}}$	0.25 old (60 years)/young (20 years) (calculated from changes in r and f)	frequency determined by transmission electron microscopy 7.7±0.7 [1/μm] (young, human), 1.5±0.4 [1/μm] (old, human), old/young 0.19 9.4±0.9 [1/μm] (young, baboon), 5.5±0.7 [1/μm] (old, baboon), old/young 0.58
endothelial thickness $\frac{y_{end}^{old}}{y_{end}^{young}}$	1.75 old (60 years)/young (20 years)	Determined by transmission electron microscopy 165±17nm (human, young), 289±9nm (human, old), old/young 1.75 130±8nm (baboon, young), 186±9nm (baboon, old), old/young 1.43

Cogger2003, Warren2005

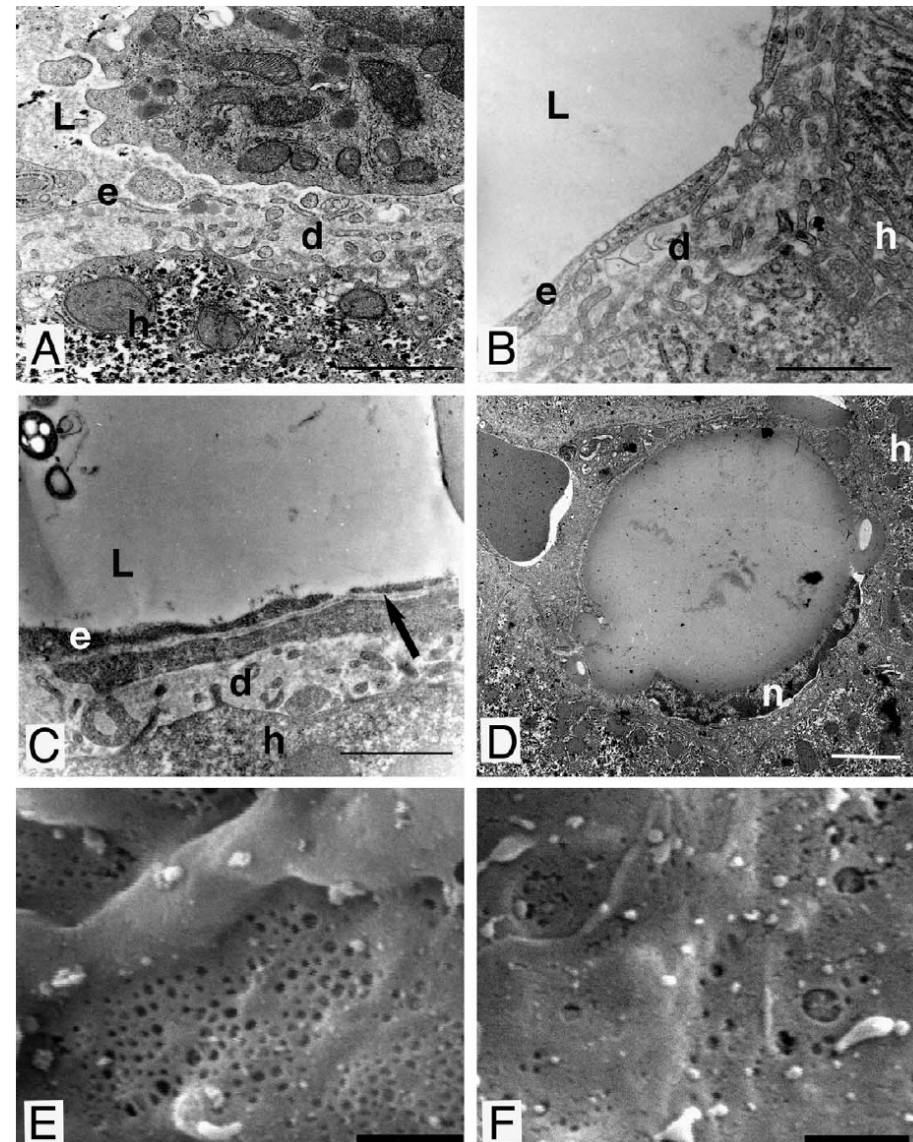
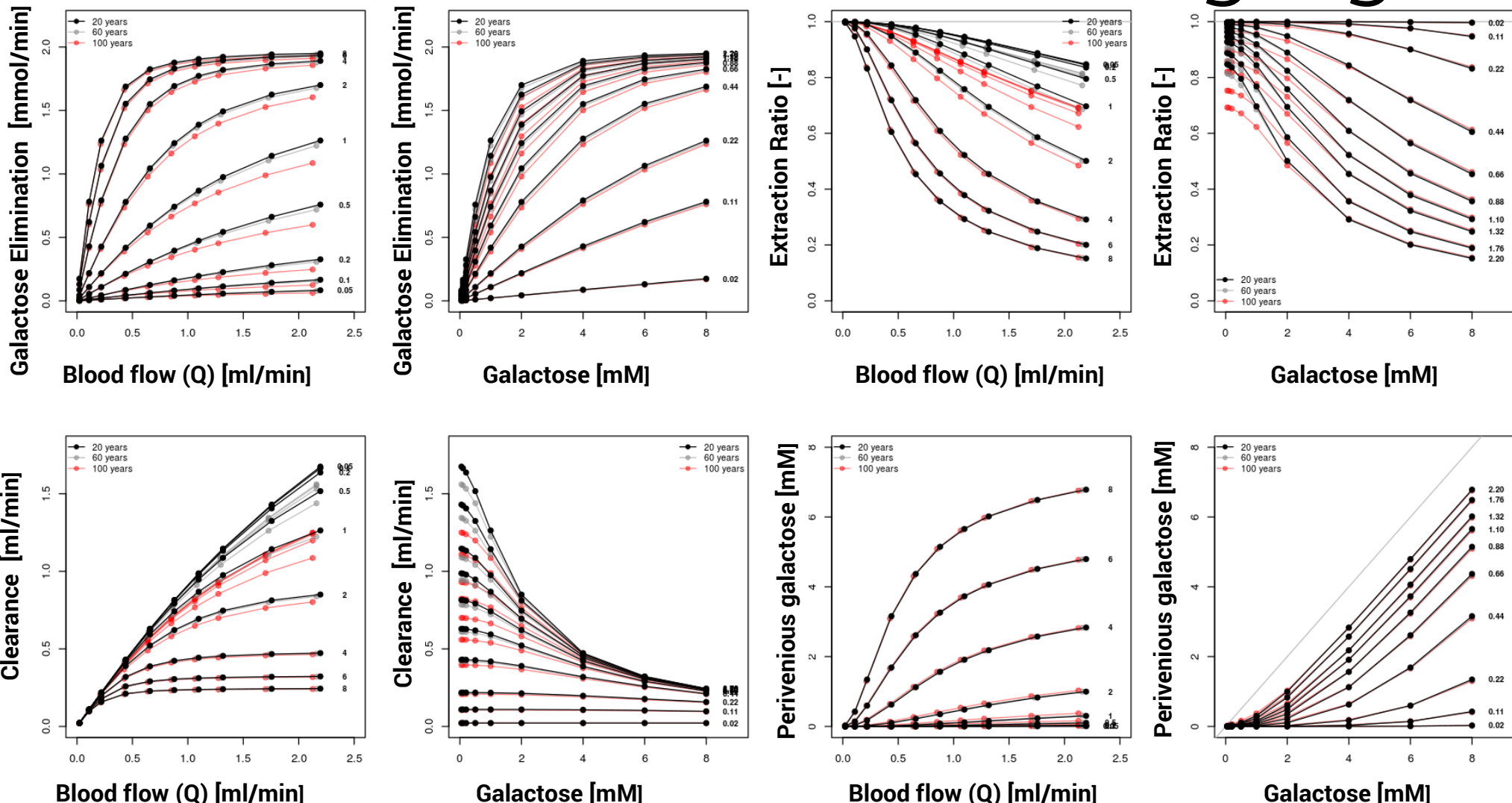


Fig. 2. Electron microscopy of the baboon liver. Transmission electron micrographs of the young (A) and old baboon liver (B–D). The endothelial cells (e) are thickened and defenestrated with old age. Increased extracellular matrix is found in the space of Disse (d) in the old livers. There is basal lamina deposition beneath the endothelial cells in some old baboons (→ (C)). A lipid laden ring-shaped cell is shown in (D). The nucleus (n) is located in the rim of cytoplasm that surrounds the lipid droplet. Scanning electron micrographs of the young (E) and old (F) liver. There is defenestration of the endothelium in the old baboons. (Abbreviations: h, hepatocyte; e, endothelial cell; L, sinusoidal lumen; n, nucleus; d, space of Disse. Scale bars: (A–C, E and F) = 1 μm, (D) = 5 μm).

Reduced Clearance in aging



- Reduced Clearance & Extraction ratio under low concentrations (local effect)
- In combination with reduced liver volume & perfusion in age can have drastic effects on drug/compound clearance

WP0 Central Data Management

<https://www.fairdomhub.org/projects/46>

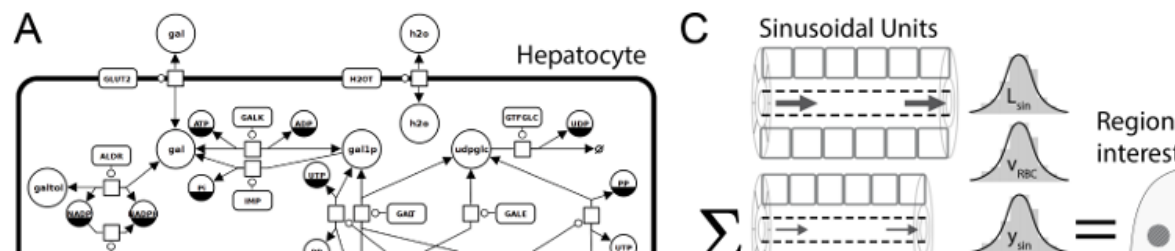
- Project & assets are managed in central data management (SEEK & fairdomhub)
- Multiple meetings/TC with data management (Heidelberg, Fairdom user meeting)
- Project Webpage setup
- Open Access (Models) & Open Source (Code) & Open Data (?)

The screenshot shows the FAIRDOM HUB interface for the LiSyM-MM-PLF project. At the top, there's a navigation bar with 'FAIRDOM HUB' logo, search bar, and user profile 'Matthias König'. Below it, the breadcrumb navigation shows 'Home / Projects Index / LiSyM-MM-PLF: Multi-Scale Models for Personalized Liver Function Tests'. The main content area has a title 'LiSyM-MM-PLF: Multi-Scale Models for Personalized Liver Function Tests' with a subtitle 'No description specified'. It lists project details: Programme (LiSyM - Systems Medicine of the Liver), Public web page (<https://livermetabolism.com>), Internal web page (Not specified), Organisms (Homo sapiens, Mus musculus, Rattus norvegicus), FAIRDOM PALs (No PALs for this Project), Project administrators (Martin Golebiowski, Wolfgang Müller, Matthias König), Asset housekeepers (No Asset housekeepers for this Project), and Asset gatekeepers (No Asset gatekeepers for this Project). To the right, there's a liver icon with a 'Change picture' link and a 'Storage Usage' section showing a total size of 709 KB. Below the main content, there's a 'Related items' section with links to People (4), Institutions (4), Investigations (2), Studies (1), Assays (1), Data files (1), Models (1), and Publications (2).

<https://www.livermetabolism.com/>
Multiscale-galactose metabolism

Multiscale model of human galactose metabolism - from single hepatocytes to individual liver function.

Model overview



Time table PLF

